CONVLUTIONAL NEURAL NETWORK BASED HYBRID PRECODING FOR CELL FREE MASSIVE MIMO SYSTEM

Yonas Negeri Jima

A Thesis Submitted to the Department of Electronics and Communication Engineering
Colleges of Electrical Engineering and Computing

Presented in Partial Fulfillment of the Requirement for the Degree of Master's in Electronics and Communication Engineering
(Specialization in Communication Engineering)

Office of Graduate Studies
Adama Science and Technology University

May, 2025
Adama, Ethiopia

CONVLUTIONAL NEURAL NETWORK BASED HYBRID PRECODING FOR CELL FREE MASSIVE MIMO SYSTEM

YONAS NEGERI JIMA

Advisors:

Dr. Demissie Jobir

Dr. Tadele Abera

A Thesis Submitted to the Department of Electronics and Communication Engineering

Colleges of Electrical Engineering and Computing

Presented in Partial Fulfillment of the Requirement for the Degree of Master's in Electronics and Communication Engineering

(Specialization in Communication Engineering)

Office of Graduate Studies
Adama Science and Technology University

May, 2025
Adama, Ethiopia

Declaration

I hereby declare that this Thesis entitled "*CNN BASED HYBRID PRECODING FOR CELL FREE MASSIVE MIMO SYSTEM"* is my original work. That is, it has not been submitted for the award of any academic degree, diploma or certificate in any other university. All sources of materials used for this thesis have been duly acknowledged through appropriate citations.

Yonas Negeri	____________	____________
Name of Student	Signature	Date

Recommendation of Advisors

we, the advisors of this Thesis, hereby certify that we have read and revised the thesis entitled "*CNN BASED HYBRID PRECODING FOR CELL FREE MASSIVE MIMO SYSTEM*" prepared under our guidance by YONAS NEGERI JIMA submitted in partial fulfillment of the requirements for the degree of master in of Science in Communication Engineering we recommend the submission of the thesis to the department for further review and defense.

Dr.Demisse Jobir	________________	_____________
Major Advisor	Signature	Date
Dr.Tadele Abera	________________	09/06/2025
Co-advisor	Signature	Date

Approval Page

We, the advisors of this Thesis, entitled "*CNN BASED HYBRID PRECODING FOR CELL FREE MASSIVE MIMO SYSTEM*" prepared under our guidance YONAS NEGERI JIMA hereby certify that the recommendation and suggestions made by the board of examiners are appropriately incorporated into the final version of the thesis.

Dr. Demisse Jobir	________________	________________
Major Advisor	Signature	Date
Dr.Tadele Abera	________________	09/06/2025
Co-advisor	Signature	Date

We, the undersigned, members of the Board of Examiners of the thesis by YONAS NEGERI JIMA have read and evaluated the thesis entitled "*CNN BASED HYBRID PRECODING FOR CELL FREE MASSIVE MIMO SYSTEM*" and examined the candidate during open defense. Therefore, to certify that the thesis is accepted for partial fulfillment of the requirement of the degree of Master of Science in Communication Engineering.

________________	________________	________________
Chairperson	Signature	Date
________________	________________	________________
Reviewer 1	Signature	Date
________________	________________	________________
Reviewer 2	Signature	Date

Final approval and acceptance of the thesis proposal is contingent upon submission of its final copy to the Office of Postgraduate Studies (OPGS) through the Department Graduate Council (DGC) and Colleges Graduate Committee (CGC).

________________	________________	________________
Department Head	Signature	Date
________________	________________	________________
Colleges Dean	Signature	Date
________________	________________	________________
Office of Postgraduate Studies, Dean	Signature	Date

ACKNOWLEDGEMENT

First and foremost, I give all glory and honor to my Lord and Savior Jesus Christ, whose grace, strength, and wisdom have guided me throughout this journey. Without His divine presence, this work would not have been possible. I would like to express my heartfelt gratitude to my main advisor, **Dr. Demissie Jobir**, for his invaluable guidance, support, and encouragement throughout the course of this research. His mentorship has been a crucial part of my academic growth. I am also sincerely thankful to my co-advisor, **Dr. Tadele Abera**, for his constructive feedback, thoughtful suggestions, and continued support that enriched this thesis. My deepest appreciation goes to my beloved parents, **Tezerash Tilahun** and **Nagari Jima,** for their endless love, prayers, and sacrifices that have carried me to this point. Their belief in me has been my foundation. A special thanks to **Meron Tesfaye** for her encouragement, kindness, and support during this academic journey. Her presence has been a source of strength and motivation. I would also like to extend my heartfelt thanks to **Workeneh Geleta** for his special support and contributions. His assistance and encouragement have meant a great deal to me throughout this journey. To everyone who contributed to this achievement in one way or another—thank you from the bottom of my heart.

Table of Contents

LIST OF TABLES

LIST OF FIGURES

Acronyms

5G	Fifth Generation
AP	Access Point
BER	Bit Error Rate
CFMM	Cell Free Massive MIMO
CNN	Convolutional Neural Network
CPU	Central Processing Unit
CSI	Channel State Information
DOA	Direction of Arrival
DOD	Direction of Departure.
DL	Deep learning
DNN	Deep neural network
EE	Energy Efficiency
FLOPS	Floating Point Operations per Second
FC	Fully Connected
ML	Machine Learning
MIMO	Massive Multiple-Input Multiple-Output
MSE	Mean Squared Error
MMSE	Minimum Mean Squared Error
MU MIMO	Multi User MIMO
RF	Radio Frequency
RZF	Regularized Zero-Forcing
SE	Spectral Efficiency
SNR	Signal-to-Noise Ratio
SNIR	Signal-to-Noise plus Interference Ratio
THz	Terahertz
UE	User Equipment
UL	Uplink
ZF	Zero forcing

ABSTRACT

Combining terahertz (THz) and cell-free massive Multiple-Input Multiple-Output (CFMM) communication technologies offers a viable solution to satisfy the high performance demands of next wireless networks. Significant advantages of this combination include reduced system complexity, increased energy efficiency, and improved spectrum efficiency. Notwithstanding these benefits, real-time signal processing and channel estimation in decentralized architectures are particularly difficult due to the dynamic and unpredictable nature of THz channels. Such rapid channel variations frequently make it difficult for conventional precoding and channel estimation approaches to react effectively. This Study presents a convolutional neural networks (CNN)*-based precoding framework created especially for CFMM systems running at THz frequencies in order to overcome this problem. The suggested approach learns the spatial and temporal features of the wireless environment to dynamically build ideal precoding weights, utilizing the potent pattern recognition powers of convolutional neural networks. This adaptive architecture lowers computing overhead while greatly improving real-time responsiveness. The model's capacity to increase spectral and energy efficiency and provide scalable, reliable performance under various network situations is confirmed by simulation results. Simulation results show that, the CNN-based strategy outperforms traditional methods in terms of energy efficiency and system complexity at a signal-to-noise ratio (SNR) of 25 dB it exhibits improved scalability and resource optimization by achieving 17 bits per joule of energy efficiency, 580 bit/s/Hz of spectral efficiency and reducing system complexity to 1,100 FLOPS. These results demonstrate an energy efficiency improvement of approximately 41.67%, a spectral efficiency gain of 10%, and a 42.11% percent reduction in computational complexity compared to the conventional MMSE precoder. These outcomes highlight the potential of CNN-driven precoding as a transformative solution for THz-enabled CFMM architectures in next-generation wireless systems*.

Keywords: Cell-free massive Multiple-Input Multiple-Output, terahertz communication, convolutional neural networks, hybrid precoding

CHAPTER ONE
INTRODUCTION

1.1 Background of the Study

Massive Multiple-Input Multiple-Output (MIMO) represents a groundbreaking advancement in wireless communication, delivering remarkable enhancements in signal quality, network capacity, and spectral efficiency. Unlike traditional MIMO systems that rely on a limited number of antennas, Massive MIMO employs a significantly larger array of antennas at both base stations and user equipment (M. B. Hassan et al., 2021).

The vast scale of these antenna arrays, sometimes reaching into the hundreds or thousands, fundamentally reshapes wireless communication by making it possible to serve multiple users at once with distinct data streams, thereby enabling highly efficient simultaneous transmissions (J. Joakim et al., 2017). This remarkable level of spatial diversity is a transformative solution, as it enables the system to more effectively separate signals, leading to a significant enhancement in overall network performance (T. Fredrik & L. Erik G, 2014).

The swift advancement of wireless communication technologies has intensified the need for faster data transmission, reduced latency, and improved energy efficiency. As we move further into the 5G era and prepare for future generations, terahertz (THz) communications are becoming increasingly critical, offering the possibility of extremely high bandwidths and exceptional data speeds. At the same time, cell-free massive multiple-input multiple-output (CFMM) systems are revolutionizing wireless networking by utilizing a widespread array of antennas to significantly boost both network coverage and overall capacity(Zhao et al., 2024)The combination of THz communication and CFMM systems is expected to address the growing demands of next-generation wireless networks. Nevertheless, merging these technologies brings significant obstacles, especially concerning energy consumption and the complexity of system design (Shoukath Ali et al., 2023).

A key breakthrough in this field is the adoption of hybrid precoding, a method designed to reduce the number of required radio frequency (RF) chains while maintaining strong sum-rate performance. This approach has become increasingly vital in high-frequency massive MIMO systems, offering an effective compromise between system efficiency and resource demands. Despite its advantages, traditional hybrid precoding techniques face significant hurdles, largely due to the substantial hardware complexity and energy consumption linked with expansive antenna arrays. These challenges highlight the urgent need for more advanced, efficient, and flexible precoding strategies (Apiyo & Izydorczyk, 2024) The computational complexity of hybrid precoding are considerably elevated, primarily due to the large-scale antenna arrays and the complexity of high-dimensional channel characteristics. Overcoming these challenges is crucial for unlocking the true capabilities of hybrid precoding, paving the way for the development of efficient and resilient communication networks in the future (Ozen & Guvensen, 2024).

CFMM represents an innovative approach to wireless communication, breaking away from the conventional structure of cellular networks. This emerging concept is built around a dense deployment of distributed access points (APs), effectively eliminating the need for traditional base stations. Equipped with multiple antennas, each access point contributes to a collective network that seamlessly provides wireless coverage (L. S. Lau & J. Joakim, 2014). Unlike conventional cellular networks where devices are limited to connecting with the nearest base station, CFMM enables mobile devices to simultaneously communicate with multiple access points, leveraging their collective spatial diversity and cooperative capabilities. This approach holds the potential to revolutionize wireless communication by significantly boosting spectral efficiency, expanding coverage, and elevating overall network performance paving the way for the deployment of 5G and future-generation networks. (C. Studer et al., 2010).

Hybrid precoding plays a crucial role in enhancing the performance of CFMM systems operating in the THz band. In massive MIMO architectures, it efficiently handles extensive antenna arrays by integrating digital and analog precoding methods, achieving an optimal trade-off among hardware complexity, energy usage, and system performance. Nonetheless, the rapidly changing channel conditions characteristic of THz communications often undermine the effectiveness of conventional hybrid precoding approaches (X. Liu, 2023).

The significance of Deep learning (DL), particularly convolutional neural networks (CNNs), in addressing challenges within these systems cannot be overstated. CNNs have proven highly effective at analyzing sequential data and capturing temporal dependencies, making them ideal for real-time prediction and adjustment to dynamic channel conditions. Their integration into the hybrid precoding process marks a key advancement in this field. The approach allows real-time adjustment of precoding weights based on current channel conditions, enhancing adaptability. This adaptability ensures the system remains practical even in the challenging THz frequency range by boosting energy efficiency and minimizing complexity. Integrating machine learning with CFMM architectures marks a major advancement in the development of next-generation wireless communication systems (Sun et al., 2023).

CNNs are highly effective for real-time prediction and adaptation in dynamic channel environments due to their ability to process sequential data and recognize temporal patterns. Leveraging live data for continuous training and updating of precoding techniques, CNNs offer enhanced adaptability and resilience compared to traditional static-model approaches, which struggle with the rapid variability typical of THz channels (Ranjith et al., 2023).

The purpose of this thesis is to Design and evaluate the performance of precoding designs based on CNN in the setting of cell free massive MIMO systems. CNNs will be used into the precoding process to create a reliable system that can adjust dynamically to changing circumstances.

1.2 Motivation of the Study

As wireless networks evolve toward 6G and beyond, there is an increasing demand for technologies that can deliver extremely high data rates, ultra-low latency, and improved energy efficiency. THz communication, when combined with CFMM architectures, offers a promising solution to meet these requirements. However, the highly dynamic nature of THz channels and the complexity of CFMM systems pose significant challenges for traditional signal processing and precoding techniques. Recent studies have demonstrated that CNNs can effectively predict hybrid precoding weights, enhancing energy efficiency and system adaptability in THz-enabled cell-free massive MIMO systems; however, the impact on spectral efficiency critical metric for high-capacity networks remains underexplored, and the effectiveness of CNN-based hybrid precoding in modeling THz channels using the Saleh-Valenzuela channel model has not been investigated. This motivates the present study to extend the existing work by analyzing the performance of CNN outputs using machine learning evaluation metrics and investigating their influence on spectral efficiency in THz-enabled CFMM systems.

1.3 Statement of the Problem

CFMM systems significantly enhance spectral efficiency (SE) and user experience, positioning them as a cornerstone for next-generation wireless communication. However, the transition to the THz band introduces critical challenges, including high path loss and complex channel dynamics, which degrade system performance and increase computational demands. Traditional hybrid precoding methods struggle to address these issues due to their reliance on computationally intensive algorithms and limited adaptability to THz-specific channel conditions. This study explores the potential of CNN-based hybrid precoding as a solution, leveraging CNNs' ability to adapt to dynamic channel variations and optimize precoding matrices. However, the effectiveness of CNN-based beamforming in mitigating high path loss and complex channel dynamics, including THz channel modeling in the Saleh-Valenzuela model, while optimizing system complexity, energy efficiency (EE), and spectral efficiency remains underexplored. Addressing this gap is crucial for the continued development and practical deployment of CF Massive MIMO systems.

1.3 Objective of the Study

1.3.1 General Objective

The general objective of this research is to analyze the performance of a CNN-based Hybrid precoding design for cell-free massive MIMO systems.

1.3.2 Specific Objectives

The specific objectives of this thesis works are as follows.

1) To develop and implement convolutional neural networks that can learn from Channel State Information (CSI).
2) To assess the CNN model's Performance in predicting hybrid precoding weights for a THz massive MIMO system using Machine Learning Metrics.
3) To analyze the effectiveness of CNN-predicted precoding weights in optimizing performance metrics such as spectral efficiency, energy efficiency, and system complexity.
4) To compare the performance of the proposed approach with state-of-the-art approaches.

1.4 Significance of the Study

This study presents an innovative hybrid precoding approach powered by CNNs, specifically designed for terahertz (THz) communication within cell-free massive MIMO (CFMM) systems. By leveraging the adaptive learning capabilities of CNNs, the proposed method dynamically adjusts precoding weights in response to rapidly fluctuating channel environments, leading to improved overall system performance. A detailed investigation into spectral efficiency reveals that the model significantly enhances data throughput and SINR across diverse THz scenarios, owing to its ability to capture spatial features of the channel with precision. Furthermore, this study addresses the critical challenge of modeling THz channels using the Saleh-Valenzuela channel model, enabling accurate representation of complex propagation characteristics such as high path loss and multipath clustering, which are essential for reliable system performance. An in-depth computational complexity evaluation demonstrates that the CNN-based framework achieves substantial reductions in processing overhead compared to conventional schemes such as Minimum Mean Squared Error (MMSE), Regularized Zero-Forcing (RZF), and Zero-Forcing (ZF). This is particularly evident in systems with large-scale antenna deployments, where the proposed method showcases strong scalability and real-time feasibility. The proposed approach also paves the way for practical deployment of THz-enabled CFMM systems in real-world 6G networks, supporting emerging applications such as holographic communications and extended reality that demand ultra-high data rates and ultra-low latency. Together with its notable gains in energy efficiency and performance validation through extensive simulations, this CNN-driven solution emerges as a promising candidate for next-generation high-frequency wireless networks, offering a balanced trade-off between complexity, adaptability, and communication reliability.

1.5 Scope of the Study

This study focuses on the design, implementation, and performance evaluation of a convolutional neural network (CNN)-based precoding approach for cell-free massive MIMO (CFMM) systems operating in the terahertz (THz) frequency band. The research specifically explores how machine learning techniques, particularly CNNs, can be used to dynamically predict optimal precoding weights by learning from spatial and temporal variations in highly dynamic THz channel environments. The study is limited to the downlink transmission scenario in a multi-user CFMM system. Key performance metrics considered include spectral efficiency, energy efficiency, computational complexity, and the prediction accuracy of the CNN model. Simulation-based evaluations are conducted to compare the proposed method against traditional hybrid precoding schemes.

1.6 Limitation of the Study

Despite the promising results, this study is not without limitations. While the proposed model demonstrates strong performance in simulation environments, its effectiveness in real-world deployments may vary due to hardware imperfections that were not fully captured in the simulated scenarios.

1.7 Thesis Organization

This thesis is organized into the following sections. **Chapter 1** outlines the study's context, research problem, objectives, key contributions, as well as its scope and limitations. **Chapter 2 concerns about literature Review** mainly focuses on overview of Cell-Free Massive MIMO System, Hybrid Precoding in THz communication, Role of Machine Learning (ML) in Wireless Communication and Review Related Work.

In fact, **Chapter 3** presents design and research methods. It mainly focuses on materials and methodology employed to conduct the research work: System modeling, Channel Modeling, Data generation and analysis, CNN-based network architecture, CNN based hybrid precoding. Finally, **Chapter 4** describes results and discussions. It mainly focuses on simulation parameters, Performance Evaluation of CNN-Based Hybrid Precoding Weight Prediction Using Machine Learning Metrics, Spectral Efficiency Comparison, Energy Efficiency Comparison, System complexity Comparison. Of course, **Chapter 5** conclusions and recommendations with potential directions for further research.

CHAPTER TWO
Literature Review

2.1 Chapter Overview

In this chapter, we review related literature on the Performance Evaluation of CNN-Based Beamforming for Cell-Free Massive MIMO Systems with a focus on mitigating hardware impairments. Specifically, the review examines how convolutional neural networks (CNNs) can optimize beamforming by addressing challenges like distorted channel state information (CSI) and hardware non-idealities such as phase noise and amplifier nonlinearities. The focus also includes the integration of higher frequency bands, particularly Terahertz (THz), and the impact of these impairments on both static and dynamic wireless environments for beyond 5G communication systems.

2.2 General Overview of Cell-Free Massive MIMO Systems

Cell-Free Massive MIMO (Multiple-Input Multiple-Output) is an emerging architecture in wireless communications that eliminates the conventional concept of cell-based coverage. Rather than dividing the service area into cells, this system uses a large number of spatially distributed, energy-efficient access points (APs) to jointly serve all users. Each user is simultaneously connected to all APs, creating a uniform service experience across the entire network. These APs are coordinated by a central processing unit, enabling streamlined transmission and resource management. This model significantly enhances spectral efficiency and reduces interference by leveraging spatial diversity. Importantly, it operates with low-complexity techniques such as linear precoding and relies on statistical channel knowledge at the transmitter. Compared to traditional small cell setups, Cell-Free MIMO offers considerable improvements in user fairness and signal quality particularly for users in less favorable locations by dramatically increasing metrics like the 5% outage rate.

When comparing Cell Free Massive MIMO with traditional small-cell networks, the advantages of the cell-free approach become clear. In small-cell configurations, each user is served by the nearest access point, leading to inconsistent service quality and challenges for users at the edge of coverage areas. Cell Free MIMO avoids these issues by allowing all APs to collaboratively transmit to all users, ensuring balanced and reliable service. Simulation results from research show that CF MIMO significantly boosts performance in key metrics like the 5% outage rate, even when using simpler power allocation methods. For instance, systems employing CB or ZF with optimized power control vastly outperform small-cell alternatives. Furthermore, as the network scales with more users and APs, the performance of CF-MIMO remains stable, whereas small-cell systems tend to degrade. This resilience and improved quality make CF-MIMO a strong candidate for future wireless infrastructure, offering a more equitable and efficient way to deliver high-speed connectivity.

2.2.1 Power Allocation and Linear Precoding in Cell-Free Systems

One of the critical challenges in Cell-Free MIMO networks is optimizing how transmission power is distributed and how signals are precoding. The system utilizes linear precoding methods such as Conjugate Beamforming (CB) and Zero Forcing (ZF) to improve signal quality and reduce interference among users. CB stands out for its simplicity, directly using estimated channels for signal transmission, making it ideal for scenarios where computational resources are limited. Optimization techniques like max-min fairness can be applied to calculate power coefficients while respecting constraints on each antenna's output power. In contrast, ZF precoding cancels interference more effectively but requires more computation and centralized coordination. Here, power allocation typically depends only on the user rather than the specific antenna. These methods enable the system to maintain strong performance and fairness across users, even in complex or dense environments. Together, they provide scalable and efficient solutions for managing resources in a large, distributed network (Nayebi et al., n.d).

2.2.2 Pilot Assignment and Interference Management in Cell-Free Systems

As Cell-Free Massive MIMO systems grow in scale, managing pilot contamination becomes essential for sustaining their performance. Pilot contamination arises when multiple users share non-orthogonal pilot sequences, resulting in inaccurate channel estimates and degraded data transmission. This issue becomes particularly challenging when the number of users exceeds the number of available orthogonal pilot sequences. To address this, two pilot assignment strategies have been proposed: random and greedy pilot assignment. While the random approach assigns pilots arbitrarily, it often results in nearby users reusing the same sequence, which amplifies interference. In contrast, the greedy pilot assignment method iteratively minimizes pilot contamination by allowing the user with the poorest performance to select a new pilot sequence that reduces overlap with others. Simulation results show that greedy assignment nearly closes the gap with the ideal case of orthogonal pilots, even when the number of available sequences is limited. Alongside intelligent pilot allocation, max-min power control schemes can be employed to further mitigate interference and ensure that all users receive a baseline level of service quality. Together, these techniques enhance the robustness and fairness of Cell-Free systems, especially in dense and heterogeneous deployments (He et al., 2021).

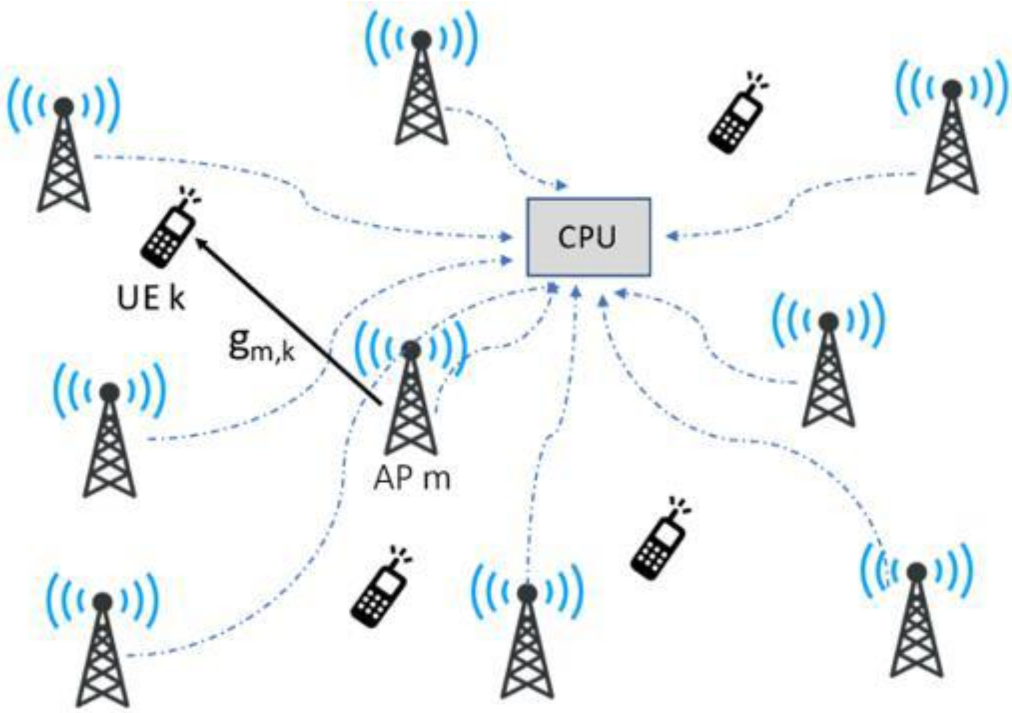

Figure 2.1 Cell-Free Massive MIMO system (Zheng Chen, 2017).

2.2.3 Advantages of Cell-Free Massive MIMO Over Traditional Cellular Architecture

The CFMIMO system is a revolutionary wireless communication architecture that differs from traditional cellular networks. Here's a breakdown of its key advantages over traditional cellular systems (Ashikhmin, 2017).

1. Uniform Quality of Service (QoS)

- In traditional cellular networks, users close to the base station (BS) receive better service than users at the edge of the cell.
- CFMIMO eliminates this by deploying a large number of distributed access points (APs) over a wide area, all serving the users cooperatively without defining cells.

2. Reduced Inter-Cell Interference

- In traditional cellular systems, interference from neighboring cells (especially at the edges) significantly degrades performance.

- In cell-free systems, **coherent joint transmission** from multiple APs minimizes this interference.

3. Improved Spectral Efficiency

- With more distributed APs, the channel hardening effect becomes more pronounced, and users benefit from improved spectral efficiency.
- Compared to small-cell or macro-cell systems, cell-free MIMO consistently outperforms in total system throughput.

2.3 Hybrid Precoding in Terahertz Communications

As the vision for sixth-generation (6G) wireless systems advances, the Terahertz (THz) frequency band is gaining recognition for its potential to meet ultra-high-speed data demands. Due to the extreme path loss in this band, communication systems must employ ultra-massive MIMO arrays with highly directional beams to maintain signal quality. Hybrid precoding, which blends analog and digital signal processing, has emerged as a promising approach in this context. It reduces the number of costly RF chains by allowing partial digital control while maintaining high performance through analog phase shifting. The focus of recent research is on the fully-connected hybrid precoding architecture, where each RF chain drives all antennas. This design, although powerful, poses challenges in terms of complexity and energy efficiency. To overcome these issues, new low-complexity algorithms like Column-by-Column (CBC) precoding are being explored, aiming to maintain high spectral efficiency while reducing the system's implementation burden.

2.3.1 Fully-Connected Hybrid Precoding

In fully-connected hybrid precoding architectures, each RF chain is linked to all transmit antennas, allowing maximum flexibility in beamforming and signal shaping. This structure enables near-optimal performance but requires complex hardware and consumes more power due to the dense network of phase shifters. The paper introduces a method to analytically approximate the spectral efficiency of this setup. This model bridges the gap between theoretical fully digital systems and practical hybrid systems by quantifying the performance loss using matrix norms. Importantly, the derived expression captures how closely a hybrid precoder can mimic a digital one, providing a solid benchmark for algorithm development. The analysis helps highlight where performance sacrifices occur and sets the stage for designing more efficient precoding strategies tailored for the THz band.

2.3.2 Partially-Connected Hybrid Precoding

To further tackle the complexity and power limitations of fully-connected architectures, partially-connected hybrid precoding has been proposed as a more hardware-efficient solution. In this design, each RF (Radio Frequency) chain is connected only to a subset of antennas, forming smaller sub-arrays. This dramatically reduces the number of required phase shifters and interconnections, leading to lower energy consumption and easier implementation. However, this simplification comes at the cost of reduced beamforming flexibility, which can degrade spectral efficiency. The challenge with partially-connected systems lies in optimizing the precoding design to extract maximum performance within the architectural constraints. Recent research focuses on developing new hybrid architectures, such as dynamic or switch-based array structures, to strike a balance between efficiency, complexity, and performance especially under the demanding conditions of THz wideband channels (Longfei Yany et al., 2022).

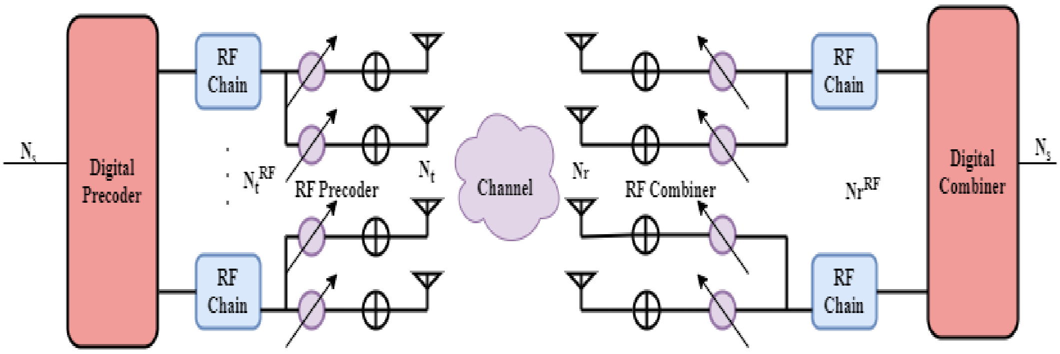

Figure 2.2 Partially Connected Hybrid Precoding (Abose et al., 2024)

2.4 Machine Learning in Wireless Networks

Machine learning (ML) is redefining the architecture and functionality of wireless networks as the industry advances toward 6G technologies. Conventional approaches, which depend on rigid mathematical frameworks and heuristic algorithms, often fall short in managing the dynamic, non-linear complexities of modern communication environments. ML introduces adaptive, data-centric methodologies that enhance real-time decision-making, automate network operations, and optimize performance across diverse scenarios. At the physical layer, ML algorithms excel in decoding intricate channel variations, mitigating synchronization errors, and improving signal integrity in environments with hardware imperfections. In the MAC layer, reinforcement learning (RL) and federated learning (FL) enable intelligent resource distribution, energy-efficient power adjustments, and proactive handling of asymmetric traffic patterns. At the application layer, ML supports autonomous network management, precise unmanned aerial vehicle (UAV) navigation, and efficient data routing in vehicular networks. Advanced techniques, such as convolutional neural networks (CNNs) and recurrent architectures (RNNs), process high-dimensional data for tasks like beamforming and anomaly detection, while FL ensures collaborative model training without compromising data privacy. Persistent challenges include limited training datasets, edge-device computational bottlenecks, and harmonizing performance with energy consumption. As 6G targets ultra-reliable connectivity for applications like industrial IoT and immersive extended reality (XR), ML's capacity for context-aware automation and robust security mechanisms underscores its indispensability in future wireless ecosystems (Ali et al., 2020).

2.4.1 Exploring Machine Learning Approaches for Beamforming in Massive MIMO Networks

This segment delves into how various machine learning paradigms perform in the context of beamforming optimization for Massive MIMO in 5G networks. It assesses four key techniques: deep learning-based approaches (DLBA), reinforcement learning-based approaches (RLBA), clustering-based algorithms (CBA), and genetic algorithm-based methods (GABA). Among these, DLBA and RLBA exhibit enhanced spectral efficiency and signal quality by harnessing spatial pattern recognition and iterative policy improvement, respectively. DLBA utilizes neural models that dynamically adapt to fluctuating channel state information, while RLBA leverages trial-and-error feedback loops to refine beamforming decisions under real-time interference. In contrast, CBA and GABA yield moderate outcomes CBA structures users into spatially coherent groups, and GABA mimics evolutionary principles to optimize performance but both face limitations in adapting swiftly to network changes. Notably, the primary bottlenecks for DLBA and RLBA are high computational demands, whereas CBA and GABA struggle with scalability in ultra-dense environments. Future innovation could lie in hybridized frameworks (e.g., combining DLBA's spatial learning with CBA's segmentation) or using meta-learning to foster model adaptability across varying deployment scenarios. This line of research aligns with broader efforts to refine physical-layer intelligence, balancing performance, response time, and system constraints for emerging 6G use cases.

2.4.2 Practical Deployment Hurdles of Machine Learning-Based Beamforming in 5G/6G Systems

Despite the theoretical promise of ML-driven beamforming, translating these techniques into operational 5G/6G networks presents tangible challenges. These include processing overhead, real-time CSI fluctuations, and hardware resource limitations, particularly at the network edge. DLBA and RLBA, while effective, are computationally intensive requiring large-scale datasets and prolonged training, which poses obstacles for low-power or latency-sensitive devices. To address these issues, the paper points to techniques like neural network compression (e.g., pruning and quantization) and hardware acceleration via FPGA or ASIC platforms as key enablers of real-time efficiency. Interestingly, while slower, GABA offers clearer logic in static or predictable scenarios, such as fixed user clusters. Going forward, distributed intelligence architectures where model training occurs collaboratively between cloud and edge—could ease these burdens. Moreover, the rise of ultra-lightweight models (such as TinyML) holds promise for delivering responsive and resource-efficient beamforming solutions. These advancements contribute to ongoing conversations around edge AI, model decentralization, and robust learning under constrained conditions. Finally, there's a growing imperative to develop standardized interfaces for ML-driven beamforming systems, ensuring consistent functionality across diverse 5G/6G hardware and software ecosystems (Upadhyay et al., 2024).

2.5 Review of Related Work

The paper (Ngo et al., 2017) highlighted the superior performance of cell-free systems in terms of spectral efficiency, consistent service quality, and resilience to user mobility when comparing cell-free massive MIMO with small cells. The authors stressed that several dispersed access points (APs) work together to serve customers in cell-free networks, reducing interference and improving signal quality. This decentralized strategy is a desirable option for upcoming wireless networks since it provides notable increases in capacity and coverage.

In the work (Kürner et al., 2013) examined the core characteristics of Terahertz wireless communication, highlighting how the integration of cell-free massive MIMO could revolutionize link performance in this spectrum. Their analysis brought attention to the inherent difficulties of accurately estimating channels at THz frequencies and proposed hybrid precoding as a viable method to streamline system architecture and minimize operational complexity.

(Elbir, 2019) presents a novel approach to hybrid beamforming in millimeter-wave (mmWave) MIMO systems using convolutional neural networks (CNNs). Unlike conventional techniques such as Orthogonal Matching Pursuit (OMP) or alternating minimization that depend on accurate steering vector knowledge and involve significant computational burdens, this work introduces a data-driven alternative. The CNN-based model is trained to infer both analog and digital precoders from imperfect channel state information (CSI), removing the need for explicit estimation of direction-of-arrival (DoA) or direction-of-departure (DoD). This architecture not only maintains near-optimal spectral efficiency but also drastically cuts down processing time. The study demonstrates that the proposed method outperforms traditional optimization and heuristic algorithms, particularly in noisy CSI environments, making it a promising candidate for real-time hybrid beamforming. However, the paper's focus remains solely on spectral efficiency, leaving other important performance indicators like energy efficiency and bit error rate (BER) unexamined.

The paper in (Huang et al., 2019) presents a novel application of deep learning to enhance hybrid precoding in mm Wave massive MIMO systems. Traditional approaches like SVD and GMD often require high computational resources and do not fully exploit the spatial characteristics of mm Wave channels, limiting their efficiency. The authors propose a deep neural network (DNN) framework that models the hybrid precoding process as an end-to-end learning task, enabling the network to directly map the input channel information to optimized precoder and combiner matrices. Extensive simulations reveal that this DNN-based method not only improves bit error ratio (BER) and spectral efficiency but also reduces computational complexity, offering a practical and effective solution for next-generation wireless systems. This work underscores the capability of deep learning to address the challenges of mm Wave MIMO systems, particularly in reducing computational overhead while maintaining high performance.

(Bendjillali et al., 2023) introduced a deep learning method for beamforming in 5G large multiple-input multiple-output (MIMO) systems, utilizing the ResNeSt architecture. By streamlining and optimizing the beamforming process, the ResNeSt-based deep learning technique enhances the effectiveness and performance of 5G and beyond communication networks. The fundamental constraints of the conventional approaches can be eliminated by maximizing channel capacity while avoiding interference, according to a research of beamforming capabilities. The suggested model outperforms conventional methods in a variety of interference circumstances and demonstrates exceptional adaptability to dynamic channel conditions. Despite there are several challenges that warrant further investigation. One such challenge is the need to scale the proposed model to handle larger antenna arrays and more complex real-world scenarios. Additionally, exploring the impact of various environmental factor.

(Elbir, 2020) proposes a Deep learning (DL) framework to address both hybrid beamforming and channel estimation. For this purpose, they introduce three deep convolutional neural network (CNN) architectures. These architectures assume that the base station (BS) has only the channel statistics and feed the channel covariance matrix into a CNN to obtain the hybrid precoders at the receiver, two CNNs are employed: one for channel estimation and another for designing the hybrid combiners. The proposed deep learning (DL) framework eliminates the need for instantaneous feedback of CSI at the base station (BS). Additionally, the online deployment of DL for channel estimation was investigated. It was shown that the proposed approach achieves higher spectral efficiency compared to conventional techniques. Furthermore, the DL framework demonstrates at least 10 times lower computational complexity than conventional optimization-based methods.

In their 2021 study,(Khalid et al., 2021) introduce an integrated deep learning framework leveraging convolutional neural networks (CNNs) to simultaneously address precoder optimization and antenna selection in a partially connected massive MIMO hybrid beamforming system. They model the precoder optimization as a regression task and antenna selection as a classification problem within the CNN architecture. Initially, the input channel information is processed by the first CNN, which identifies the most efficient subset of antennas to maximize spectral efficiency. This selected antenna subset is then passed to a second CNN, responsible for generating the block-diagonal precoder aligned with the partially connected hardware topology. Comparative simulations affirm that this dual-CNN approach surpasses traditional methods such as iterative algorithms and alternating minimization in terms of both efficiency and performance.

(Sallam & Attiya, 2021) propose a convolutional neural network (CNN)-driven solution for real-time two-dimensional adaptive beamforming in phased array systems, aiming to mitigate the effects of computational overhead and hardware imperfections. The CNN is pre-trained using datasets generated from the Wiener beamforming method and is capable of predicting beamforming weight vectors with high precision. Notably, the model maintains strong performance in the presence of array distortions such as mutual coupling and phase mismatches. When benchmarked against radial basis function neural networks (RBFNN), the CNN achieves better pattern fidelity and interference rejection. Despite its strengths in adaptability and accuracy, the method depends heavily on comprehensive offline training and adopts simplified assumptions regarding real-world array imperfections. Additionally, improvements in hardware acceleration would be necessary to fully enable its use in time-sensitive applications.

(Huttunen et al., 2022) explore the application of deep fully convolutional neural networks (CNNs) in receiver side processing and report notable performance gains. Building on this foundation, their study extends the use of machine learning to the transmitter side specifically focusing on CNN-based beamforming. The proposed model takes uplink channel estimates as input and predicts downlink channel conditions, enabling more efficient beamforming strategies. This supervised learning framework is carefully designed to optimize the end-user experience by incorporating a loss function that reflects receiver-side performance metrics. The core objective of the CNN is to model and track the transformation of channels between uplink and downlink transmissions, correcting for imperfections across the signal processing pipeline, including the beamforming stage. Simulations reveal that this approach significantly boosts beamforming accuracy. Although the findings are especially pertinent to ongoing research in CNN-assisted beamforming for cell-free massive MIMO setups, the study does not address hybrid beamforming architectures an omission that limits its applicability to high-frequency and large-scale systems such as those operating in the THz band, where balancing hardware efficiency and performance is crucial.

(J. Zhang et al., 2023) investigate deep learning techniques to predict transmit beamforming using only historical channel data, without relying on current channel information, in the multiuser multiple-input-single-output (MISO) downlink. This approach significantly reduces channel estimation overhead and improves spectrum efficiency, particularly in high-mobility vehicular communications. Specifically, they propose a joint learning framework that integrates channel prediction and power optimization to directly predict transmit beamforming. The proposed predictive beamforming scheme significantly enhances effective spectrum efficiency compared to traditional channel estimation methods and those that separately predict the channel and then optimize beamforming.

(Venkatesh Tentu; & Dheeraj Naidu Amudala, 2020) investigate the role of convolutional neural networks (CNNs) in enabling adaptive hybrid precoding for millimeter-wave MIMO systems—a foundational technology for the evolution toward more advanced Terahertz (THz) communication frameworks. The study proposes a dynamic CNN-based method that intelligently adjusts the hybrid precoding matrices in real time, optimizing the coordination between digital and analog signal processing components. This adaptive approach is designed to enhance transmission efficiency while maintaining a balance between performance and hardware limitations. Through extensive simulation-based evaluation, the authors demonstrate that the proposed framework excels in terms of both energy efficiency and system manageability, highlighting its strong potential for scalable deployment in next-generation high-frequency wireless networks.

(Abugubba et al., 2022) introduced a convolutional neural network (CNN)-based hybrid precoding approach tailored for millimeter-wave massive MIMO systems, demonstrating that it can nearly match the performance of fully digital precoding while offering significantly lower computational complexity. The proposed method illustrates how deep learning can effectively optimize beamforming strategies and shows strong alignment with conventional benchmarks through simulation-based evaluation. However, the exclusive dependence on simulated environments brings into question the model's generalizability to real world deployments. Additionally, the study does not explore the model’s performance under diverse or fluctuating channel conditions. To bridge these gaps, future investigations should examine the framework’s behavior in practical scenarios and consider the adoption of alternative deep learning methods to further strengthen adaptability and resilience in dynamic wireless settings.

(Nguyen et al., 2019) investigated strategies for enhancing energy efficiency in two-way amplify-and-forward (AF) half-duplex MIMO relay systems, where several user pairs communicate via a common relay node. Departing from traditional iterative optimization techniques, the study introduced a deep neural network (DNN)-based solution specifically for the uplink scenario. The proposed model effectively captured the complex relationships in the system and achieved near-optimal energy efficiency. This deep learning-based approach outperformed conventional iterative algorithms, showcasing the potential of neural networks in solving complex resource allocation problems in MIMO relay environments.

(Khan et al., 2020)pioneered the foundational analysis of cell-free massive MIMO (CFMM) systems, providing analytical insights through the derivation of explicit closed-form expressions. Their primary focus was on optimizing energy efficiency, which they approached using a structured two-phase methodology. Initially, the energy optimization task was reformulated as a convex problem, ensuring tractable and reliable convergence. In the subsequent phase, the solution was derived in a distributed fashion by leveraging the method of multipliers an iterative technique well-suited for decentralized processing in large-scale systems. This strategy not only enhanced energy performance but also enabled practical implementation across geographically dispersed access points, making it highly relevant for scalable next-generation wireless networks.

(Abose et al., 2024b) provided an in-depth analysis of energy efficiency (EE) and system complexity for CNN based hybrid precoding in cell-free massive multiple-input multiple-output (CFMM) systems operating in the terahertz (THz) band. However, the spectral efficiency (SE) of this approach under THz conditions remains unexplored. Given the critical trade-offs between SE, EE, and system complexity in high-frequency, high-capacity networks, further investigation into SE is essential. While their study employs a THz-specific clustered channel model to capture the propagation characteristics of THz frequencies, the current research adopts the Saleh-Valenzuela model, which may offer different insights into channel dynamics and precoding performance.

2.5.1 Research Gap Analysis

The literature showcases notable progress in CNN-based hybrid precoding for mm Wave and MIMO systems, achieving improvements in spectral efficiency, energy efficiency, and reduced computational complexity. However, most studies are limited to mm Wave frequencies and rely heavily on simulations, with minimal focus on the more demanding Terahertz (THz) spectrum. Additionally, existing works often analyze spectral or energy efficiency in isolation, without offering a comprehensive evaluation that includes computational complexity. While there are studies explore CNN-based approaches in cell-free massive MIMO systems under THz-specific clustered channel scenarios, they typically lack a unified assessment of all three key metrics. This creates a research gap that this study addresses by focusing on CNN based hybrid precoding in THz communication, with a joint analysis of spectral efficiency, energy efficiency, and computational complexity and The current study adopts the Saleh-Valenzuela model, potentially offering different channel dynamics insights.

Table 2.1 Contribution and gap of different related works.

Title and Author	Contribution	Gap
Deep Learning for Hybrid Beamforming and Channel Estimation (Elbir, 2020)	Proposes a DL framework with three CNN architectures for hybrid beamforming and channel estimation, using channel statistics to eliminate instantaneous CSI feedback. Achieves higher spectral efficiency and lower complexity than traditional methods.	It does not address energy efficiency or performance in THz bands, limiting its relevance to high-frequency, energy-constrained systems.

Title and Author	Contribution	Gap
CNN-Based Beamforming for Downlink Prediction (Huttunen et al., 2022)	Extends CNN use to transmitter-side beamforming, predicting downlink channels from uplink estimates to optimize end-user performance. Improves beamforming accuracy in cell-free MIMO setups.	Does not address hybrid beamforming or THz band applications, limiting its relevance to high-frequency, large-scale systems requiring hardware efficiency
CNN-Based Adaptive Hybrid Precoding in mm Wave MIMO (Venkatesh Tentu & Dheeraj Naidu Amudala, 2020)	Introduces a CNN-based method for adaptive hybrid precoding in mm Wave MIMO, dynamically adjusting precoding matrices to enhance transmission efficiency and manageability. Shows scalability for high-frequency networks	Limited to mm Wave systems, with no exploration of THz or cell-free architectures, restricting insights into ultra-high-frequency, distributed systems.
CNN-Based Hybrid Precoding in mmWave MIMO (Abugubba et al., 2022)	Proposes a CNN-based hybrid precoding approach for mm Wave MIMO, achieving near-fully digital performance with lower complexity. Validates effectiveness through simulations	Does not explore diverse channel conditions or THz applications, limiting real-world adaptability.
DNN-Based Energy Efficiency in MIMO Relay Systems (Nguyen et al., 2019)	Introduces a DNN-based approach for uplink energy efficiency in two-way AF half-duplex MIMO relay systems, outperforming iterative optimization methods.	It focuses on relay systems, with no exploration of cell-free or THz architectures, limiting its applicability to distributed, high-frequency networks.
Energy Efficiency Optimization in CFMM (Khan et al., 2020)	Provides closed-form expressions for energy efficiency in CFMM systems, using a two-phase convex optimization approach solved via the method of multipliers. Enhances scalability for distributed systems	Does not address spectral efficiency or machine learning-based precoding, limiting insights into comprehensive performance optimization in THz environments.
Energy Efficiency analysis of CNN-Based Hybrid Precoding in THz (Abose et al., 2024)	Analyzes energy efficiency and system complexity of CNN-based hybrid precoding in THz CFMM systems using a THz-specific clustered channel model. Demonstrates superior performance over traditional methods.	Does not explore spectral efficiency, a critical metric for high-capacity networks.

CHAPTER THREE
MATERIALS AND METHODS

3.1 Chapter Overview

This chapter presents the system model and the proposed CNN-based hybrid precoding methodology for cell-free massive MIMO systems operating at terahertz (THz) frequencies. First, we describe the overall system architecture, including the network configuration, the channel model, and the hybrid analog-digital precoding structure under practical hardware constraints. Next, we formulate the hybrid precoding design problem with the objectives of enhancing spectral efficiency (SE), improving energy efficiency (EE), and reducing computational complexity. To address the high-dimensional optimization challenges, a convolutional neural network (CNN) is proposed to learn efficient hybrid precoding strategies based on channel state information (CSI). The architecture of the CNN, the training process, and the mapping of CNN outputs to feasible precoders are detailed. Finally, the computational complexity of the proposed method is analyzed and compared with conventional approaches.

3.2 System model

This study investigates a Cell-Free massive MIMO system designed to serve multiple users, employing a partially connected hybrid precoding architecture. We formulate the system model for the downlink which means from access points (APs) to users, as illustrated in the figures 3.1

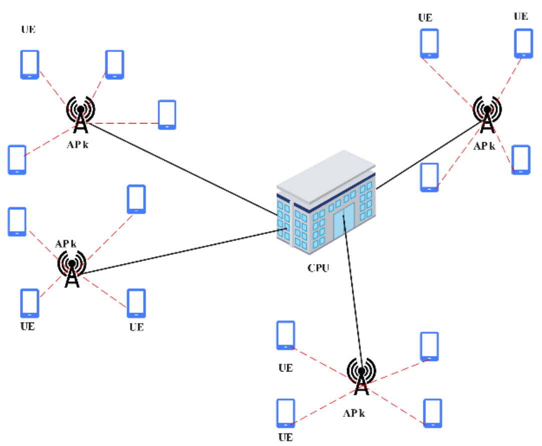

Figure 3.1 Cell-free massive MIMO architecture.

Within CFMM systems, each access point is outfitted with N_{TR} antennas and K_RF chains to serve K mobile stations (MS). On the other hand, every MS has an RF chain and N_{RT} antennas. N_{TR} Antennas using N_c data stream to communicate with N_{RT} Each AP uses a digital baseband precoder, represented by $V_B^{\dagger} = [V_{B1}{}^{\dagger}, ...V_{B_K}^{\dagger}]$ of size $\mathbf{K} \times \mathbf{K}$ within CFMM, which does away with conventional cell boundaries. This is followed by an analog precoder, V_R provides the analog precoding matrix V_R which satisfies the constant modulus constraint. Given by Equation (1)

$$V_R^{\dagger} = [V_{R1}{}^{\dagger}, ...V_{R_K}^{\dagger}] \tag{3.1}$$

Were, $V_B^{\dagger}$, $V_{B1}{}^{\dagger}$ and $V_{B_K}^{\dagger}$ represent analog precoder.

Constant modulus requirements are met by normalizing the analog precoding matrix $V_R^{\dagger}$ components. $\left|\left(V_R^{\dagger}\right)_{i,j}\right| = \frac{1}{\sqrt{N_{TR}}}$, $\forall i, j$ Let S_k' indicate the signal that was sent to the AP for the kth mobile station, and $S' = [S_1' \ ,......S_k' \ ]^T \in \mathbb{C}^{k*1}$ Thus, at the access points (APs), the transmitted signal x is expressed by:

$$x' = \sum_{k=1}^{k} V_k^{\dagger} S' \tag{3.2}$$

Where, $V_k^{\dagger} = V_R^{\dagger} V_{B_K}^{\dagger}$, $V_k^{\dagger} = [V_1, ...V_k^{\dagger}] \in \mathbb{C}^{N_{TR}*\mathrm{k}}$ represent the hybrid precoding matrices.

At kth user terminal the signal can be represented as shown in 3.3

$$y_k' = \sqrt{P_k'} V_R^{\dagger} V_{(B_k)}^{\dagger} H_k S_k' + H_k \sum_{k \neq j}^{k} \sqrt{P_j'} V_R^{\dagger} V_{B_j}^{\dagger} S_j' + n_k \tag{3.3}$$

At the KTh user terminal, the signal is combined and shown as:

$$Z_k' = W_R^H \sqrt{P_k'} V_R^{\dagger} V_{B_k}^{\dagger} H_k S_k' + H_k \sum_{k \neq j}^{k} \sqrt{P_j'} V_R^{\dagger} V_{B_j}^{\dagger} S_j' + W_R^H n_k \tag{3.4}$$

Where the THz channel from APs to the k_th user is represented by H_k dimension $N_{TR} * N_{RT}$ analog combiner at the k_th user terminal is represented by $W_R^H \in \mathbb{C}^{1*N_{TR}}$ and n_k is the noise of the receiver, which is assumed to be Gaussian distributed with zero variance and mean. $\sigma^2\mathbf{I}$ the effective channel gain for the k_th user terminal is calculated using.

$$h_{eff} = W_R^H V_R^{\dagger} H_k \tag{3.5}$$

The power of the intended signal received at the user terminal normalized by total interference is considered when calculating the signal-to-interference-plus-noise ratio (SINR) in the context of CFMM. As well as noise power (Y. Zhang et al., 2022a).

$$SINR_k = \frac{\frac{P^{'}}{K}\left|h_{eff}V_{B_k}^{\dagger}\right|^2}{\sum_{k \neq j}^{k} \frac{P^{'}}{K}\left|h_{eff}V_{B_k}^{\dagger}\right|^2 + \sigma^2} \tag{3.6}$$

As a function of SINR, the possible data rate R_k for the kth user terminal is represented by the sum rate R_k for the Kth user terminal, which is given by.

$$R_k = \log(1 + SINR_k) \tag{3.7}$$

3.3 Hybrid Precoding Optimization in Multi-User Large MIMO Systems

In multi-user large MIMO systems, hybrid precoding is usually presented as an optimization issue where the goal is to maximize the sum-rate for all users. According to (Hojatian et al., 2021), a balance between digital and analog precoding is required to guarantee effective data transmission inside the network.

To do this, an optimization model that combines digital and analog precoding methods has been created with the goal of optimizing the sum-rate of the system. Equation (3.8) formalizes this optimization procedure. This breaks down hybrid precoding into three primary parts: the digital precoder $V_{B_k}^{\dagger}$, the analog combiner W_R^H and the analog precoder $V_R^{\dagger}$. This breakdown is essential for energy economy, system performance optimization, and scalability, especially in cell-free massive MIMO systems running at THz frequencies.

3.3.1 Problem Formulation

The optimization of hybrid precoding can be mathematically expressed as

$$\begin{aligned}
&\max_{W_R V_B^{\dagger} V_R^{\dagger}} = \sum_{k=1}^{K} \log_2(1 + SINR_k) \\
&C_1 : \left|\left(V_R^{\dagger}\right)_{i,j}\right| = \frac{1}{\sqrt{N_{TR}}}, \forall i, j \\
&C_2 : \left|\left(W_R\right)_{i,j}\right| = \frac{1}{\sqrt{N_{TR}}}, \forall i, k \\
&C_3 : \left\|V_k^{\dagger}\right\|_F^2 = K
\end{aligned} \tag{3.8}$$

Breaking down hybrid precoding into separate analog and digital modules enhances processing efficiency by assigning computationally intensive tasks to the domains best suited to handle them. In massive MIMO systems, directly addressing nonconvex optimization problems is often impractical due to their high computational demands. This issue becomes even more pronounced in terahertz (THz) communications, where hybrid precoding is essential for balancing system complexity and performance. Within this framework, the analog precoder $V_R^{\dagger}$ and analog combiner W_R operate in the radio frequency (RF) domain, where they are chiefly responsible for beam steering and signal direction, all while conforming to the limitations imposed by RF hardware The constant modulus criterion, as given by $\left|\left(V_R^{\dagger}\right)_{i,j}\right| = \frac{1}{\sqrt{N_{TR}}}, \forall i, j$ this approach guarantees uniform power allocation across all antenna elements, thereby enhancing energy efficiency. Although it imposes certain limitations on adaptability, it ensures reliable signal propagation and markedly lowers computational overhead.

At the radio frequency (RF) level, analog precoding is responsible for beamforming under constant modulus constraints, offering energy-efficient operation and scalable control of large antenna arrays with minimal computational burden. In contrast, digital precoding at the baseband dynamically fine-tunes both amplitude and phase, enabling real-time signal adjustments that improve quality through precise directionality and interference mitigation. By combining these complementary capabilities, hybrid precoding strikes an effective balance between processing complexity, energy consumption, and communication performance, positioning it as a foundational technique for future wireless systems.

According to (Ammar et al., 2022), directly deriving a solution to the nonconvex optimization problem is not feasible due to its inherent complexity. However, a structured methodology can be formulated by decomposing the problem into separate analog and digital components. In the context of multi-user massive MIMO systems, this approach yields an effective equivalent channel representation, $h_{eff} = W_R^H V_R^{\dagger} H_k^{'}$ which serves as a practical strategy for simplifying the optimization task. This decomposition not only streamlines the computational process but also contributes to overall system performance. The corresponding equation delineates the constraints applied to the analog precoder echoing earlier discussions and highlights the importance of adopting a well-organized hybrid precoding framework.

$$\begin{aligned} &\max_{V_R^{\dagger} W_R} \sum_{k=1}^{K} \left\| W_R^H V_R^{\dagger} H_k \right\|_F^2 \\ &C_1 : \left|\left(V_R^{\dagger}\right)_{i,j}\right| = \frac{1}{\sqrt{N_{TR}}}, \forall i, j \\ &C_2 : \left|\left(W_R\right)_{i,j}\right| = \frac{1}{\sqrt{N_{TR}}}, \forall i, k \end{aligned} \tag{3.9}$$

In this case, the majority of beamforming activities that are computationally demanding but necessary for maximizing total signal gain are handled by the analog precoder and combiner. The optimization problem for the digital precoder is captured by Equation (3.10).

$$\max_{V_{B_k}^{\dagger}} \sum_{k=1}^{K} R_k$$
$$C_1 : \left\| V_k^{\dagger} \right\|_F^2 = K \tag{3.10}$$

This enables the digital precoding component to concentrate on maximizing the sum-rate for every user, guaranteeing that the signal is received by each user in accordance with current circumstances. The precoding hybrid method in cell-free massive MIMO systems breaks down Equation 10 into analog and digital components to maximize performance and energy efficiency. While digital precoding refines signals at the baseband to maximize signal-to-interference-plus-noise ratio and improve data speeds, analog precoding, which operates at the RF level, controls beamforming and lowers power consumption by minimizing the number of RF chains required. Particularly in high-frequency THz communication situations, this breakdown makes the system easier to construct and scale by simplifying the computing complexity.

3.4 The Minimum Mean Squared Error (MMSE) based hybrid precoding Design for downlink MU massive MIMO system

Analog Precoder and Combiner Design

The Minimum Mean Squared Error (MMSE) criterion is widely employed to minimize the mean squared error (MSE) between the transmitted signal and the received signal at mobile stations. This criterion aims to reduce the expectation:$\mathbb{E}[\|s - z\|^2]$ where S represents the transmitted signal, and Z denotes the received signal. When Channel State Information (CSI) **is** fully available, it enables the derivation of a closed-form MMSE-based analog precoder for the k-th mobile station (MS) (F. Liu et al., 2023). The overall hybrid precoding optimization problem is formulated as:

$$A_k^{MMSE} = ((H_k)^H H_k + \frac{(K\sigma^2)}{P'} I)^{-1} (H_k)^H \tag{3.11}$$

Where $H_k^{'}$ represents the channel matrix for the k-th user, $P^{'}$ indicates the transmit power, σ^2 denotes noise variance, and **I** signify the identity matrix. The analog precoder in MMSE-based systems relies on accurate channel knowledge to mitigate noise effects and improve signal quality. The analog precoder matrix is expressed as:

$$V_{R_k}^{\dagger}(i,j) = \frac{1}{\sqrt{N_{TR}}} \exp(j\theta_{i,j}) \tag{3.12}$$

Where $\theta_{i,j}$ represents the phase, shift applied to the $(i,j)^{th}$element. The effective channel matrix considering the analog precoder is then given by:

$$B_k^{\dagger} = H_k V_R^{\dagger} \tag{3.12}$$

The RF combiner G_K^{MMSE} designed using the MMSE criterion, is formulated as:

$$G_K^{MMSE} = ((B_k^{\dagger})^H B_k^{\dagger} + \frac{(K\sigma^2)}{P^{'}} I)^{-1} (B_k^{\dagger})^H \tag{3.14}$$

Which optimizes the received signal at the mobile station. The analog combiner can be written as:

$$W_R(i,j) = \frac{1}{\sqrt{N_{TR}}} \exp(j\psi_{i,j}) \tag{3.15}$$

Where denotes $\psi_{i,j}$ the phase of the $(i,j)^{th}$ element of $G_K^{\dagger}$ after applying the analog precoder and combiner, the effective channel is given by:

$$h_{eff} = W_R^H V_R^{\dagger} H_k \tag{3.16}$$

Digital Precoder Design

The goal of the analog precoder is to maximize antenna array gain. However, to further manage interference among users and refine signal transmission, a digital precoder is designed based on the MMSE criterion. Given the analog precoder $V_R^{\dagger}$ the channel matrix $H_k^{'}$ and the RF combiner W_R the MMSE-based digital precoder is:

$$V_B^{\dagger} = (h_{eff}^H h_{eff} + \frac{(K\sigma^2)}{P^{'}} I)^{-1} h_{eff}^H \tag{3.17}$$

Where h_{eff} is the effective channel after analog precoding and combining to ensure power constraints are satisfied, the normalized digital precoder for the $K\ th$ user is given by

$$(\hat{V}_{B_k}^{\dagger}) = \frac{V_{B_k}^{\dagger}\sqrt{K}}{\left\|V_R^{\dagger} V_{B_k}^{\dagger}\right\| F} \tag{3.18}$$

3.5 The Regularized Zero-Forcing (RZF) based hybrid precoding Design for downlink MU massive MIMO system

Analog Precoder and Combiner Design

Regularized Zero-Forcing (RZF) precoding balances interference suppression and noise amplification by introducing a regularization term, making it more robust than ZF the RZF precoder incorporates a regularization term to stabilize the matrix inversion, The RZF-based analog precoder matrix.

$$A_k^{RZF} = H^H (HH^H + \alpha I)^{-1} \tag{3.19}$$

The Analog Precoder $V_R^{\dagger}$ is contracted by extracting the phase angle of A_k^{RZF}

$$V_{R_k}^{RZF}(i,j) = \frac{1}{\sqrt{N_{TR}}}\exp(j\theta_{i,j}), \quad \theta_{i,j} = \angle A_K^{RZF}(i,j) \tag{3.20}$$

Here $\theta_{i,j}$ is the phase of the $(i,j)th$ element of A_k^{RZF}, ensuring that the magnitude each element is normalized to $\frac{1}{\sqrt{N_{TR}}}$ After designing the analog precoder, the effective channel is computed as :

$$B_k^{RZF} = H_k V_R^{RZF} \tag{3.21}$$

The RF combiner G_K^{RZF} designed using the RZF criterion, is formulated as:

$$G_k^{RZF} = (B^{RZF})^H (B^{RZF}(B^{RZF})^H + \alpha I)^{-1} \tag{3.22}$$

The Analog Combiner $W_R^{RZF}(i,j)$ is contracted by extracting the phase angle of G_k^{RZF}

$$W_R^{RZF}(i,j) = \frac{1}{\sqrt{N_{TR}}}\exp(j\psi_{i,j}), \quad \psi_{i,j} = \angle G_K^{RZF}(i,j) \tag{3.23}$$

Here, $\psi_{i,j}$ is the phase of the $(i,j)th$ element of G_k^{RZF}, ensuring that the magnitude each element is normalized to $\frac{1}{\sqrt{N_{TR}}}$ the effective channel is given by:

$$h_{eff} = W_R^H V_R^{\dagger} H_k \tag{3.24}$$

Digital Precoder Design

The analog precoder aims to optimize antenna array gain. To address inter-user interference more effectively and improve signal quality, the digital precoder is subsequently formulated using the Regularized Zero-Forcing (RZF) criterion. Leveraging the existing analog precoder configuration, the channel state information (represented by the channel matrix), and the RF combiner design, the RZF based digital precoder serves as the foundational framework for refining the transmission scheme.

$$V_B^{RZF} = h_{eff}(h_{eff} h_{eff}^H + \alpha I)^{-1} \tag{3.25}$$

Where h_{eff} is the effective channel after analog precoding and combining to ensure power constraints are satisfied, the normalized digital precoder for the $K-th$ user is given by

$$(\hat{V}_{B_k}^{RZF}) = \frac{V_{B_k}^{RZF}\sqrt{K}}{\left\| V_R^{RZF} V_{B_k}^{RZF} \right\| F} \tag{3.26}$$

3.6 The Zero forcing (ZF) based hybrid precoding Design for downlink MU massive MIMO system

Analog Precoder and Combiner Design

Zero forcing (ZF) precoding is aim to eliminate inter user interference by ensuring the signal received by k users from other users signal ($j \neq k$) is zero under perfect CSI the ZF analog precoder can formulated similarly to MMSE and RZF approach by modifying the precoder matrix is to focus to interference nulling

The ZF precoding matrix is based on the pseudo- inverse of channel matrix For K users the ZF -based analog precoder matrix is:

$$A_k^{ZF} = H_k^H (H_k H_k^H)^{-1} \tag{3.27}$$

Since A_k^{ZF} dose not inherently satisfy the constant modulus constraint $\left|\left(V_R^{ZF}\right)_{i,j}\right| = \frac{1}{\sqrt{N_{TR}}}$, analog Precoder V_R^{RZF} is contracted by extracting the phase angle of A_k^{ZF} .

$$V_{R_k}^{RZF}(i,j) = \frac{1}{\sqrt{N_{TR}}} \exp(j\theta_{i,j}), \quad \theta_{i,j} = \angle A_K^{RZF}(i,j) \tag{3.28}$$

Here $\theta_{i,j}$ is the phase of the $(i,j)th$ element of A_k^{ZF} , after designing the analog precoder, the effective channel is computed as:

$$B_k^{ZF} = H_k V_R^{ZF} \tag{3.29}$$

The RF combiner G_K^{ZF} designed using the ZF criterion, is formulated as:

$$G_k^{ZF} = (B^{ZF})^H (B^{ZF} (B^{ZF})^H)^{-1} \tag{3.30}$$

The Analog Combiner $W_R^{ZF}(i,j)$ is contracted by extracting the phase angle of G_k^{RZF}

$$W_R^{ZF}(i,j) = \frac{1}{\sqrt{N_{TR}}} \exp(j\psi_{i,j}), \quad \psi_{i,j} = \angle G_K^{ZF}(i,j) \tag{3.31}$$

Here $\psi_{i,j}$ is the phase of the $(i,j)th$ element of G_k^{ZF} , ensuring that the magnitude each element is normalized to $\frac{1}{\sqrt{N_{TR}}}$ the effective channel is given by:

$$h_{eff} = W_R^H V_R^{\dagger} H_k \tag{3.32}$$

Digital Precoder Design

The analog precoder is designed to maximize antenna array gain. To eliminate inter-user interference and enhance spatial multiplexing, the digital precoder is derived using the Zero-Forcing (ZF) criterion. Based on the analog precoder configuration, the channel matrix, and the RF combiner, the ZF-based digital precoder is initialized as:

$$V_B^{ZF} = h_{eff}(h_{eff} h_{eff}^H)^{-1} \tag{3.33}$$

Where h_{eff} is the effective channel after analog precoding and combining. To ensure power constraints are satisfied, the normalized digital precoder for the $K\ th$ user is given by:

$$(\hat{V}_{B_k}^{ZF}) = \frac{V_{B_k}^{ZF}\sqrt{K}}{\left\| V_R^{ZF} V_{B_k}^{ZF} \right\| F} \tag{3.34}$$

3.7 Channel Model

THz signals propagate mostly in line of sight due to their short wavelength, which causes significant attenuation and limited scattering during transmission. In order to overcome the unique propagation difficulties at THz frequencies, including acute path loss and noticeable absorption, to address this, the methodology adopted in this work employs an augmented version of the Saleh-Valenzuela model, which structures the channel into N_c distinct scattering clusters. Each cluster encompasses N_{ray} individual propagation paths. As a result, the narrowband clustered channel matrix $H \in \mathbb{C}^{N_t * N_r}$ can be mathematically formulated as (Abugubba et al., 2022).

$$H = \sqrt{\frac{N_t N_r}{N_c N_{ray}}} \sum_{i=1}^{N_c} \sum_{j=1}^{N_{ray}} \alpha_{ij} \partial_r(\phi_{ij}^r, \theta_{ij}^r) \partial_t(\phi_{ij}^t, \theta_{ij}^t)^H \tag{3.35}$$

Where, α_{ij} denotes the composite amplitude (complex-valued) of the $j-th$ propagation path within the $i\ th$ scattering cluster. The angles $(\phi_{ij}^r, \theta_{ij}^r)$ and $(\phi_{ij}^t, \theta_{ij}^t)$ represent the transmitter and receiver angular orientations, specified in the horizontal (azimuth) and vertical (elevation) dimensions, respectively. Additionally, ∂_t and ∂_r correspond to the unit-norm antenna pattern vectors at the transmitter and receiver ends, mathematically defined for the $j-th$ ray in the $i-th$ cluster the beamforming capability in both horizontal (azimuth) and vertical (elevation) spatial dimensions is achieved through a uniform planar array (UPA) configuration. This antenna architecture features a radiation pattern vector defined mathematically as:

$$\partial_{UPA}(\phi,\theta) = \frac{1}{N}\left[1,....,e^{jkd(m\sin(\phi)\sin(\theta)+n\cos(\theta))},.....,e^{jkd((N_1-1)\sin(\phi)\sin(\theta)+(N_2-1)\cos(\theta))}\right]^T \tag{3.36}$$

In this formulation, $k = \frac{2\pi}{\lambda}$ represents the wave number (spatial frequency), where d denotes the inter-element spacing between adjacent antennas. The UPA configuration comprises $N = N_1 N_2$ total elements arranged in a two-dimensional grid layout. The integer indices m and n, bounded by $0 \le m \le N_1$ and $0 \le n \le N_2$, uniquely identify the positional coordinates of each radiating element within the array structure.

3.8 Data Generation and Data Analysis

3.8.1 Data Generation

The MIMO Wireless Channel Dataset sourced from Kaggle's "MIMO Wireless Channel Dataset" framework, was generated using a THz MIMO channel simulator tailored for CNN-based hybrid precoding in terahertz CF-MMIMO systems. The dataset includes features: channel state information (CSI) components (channel gains real, channel gains imaginary, channel phases real, channel phases imaginary), spatial correlation (spatial correlation), propagation effects (path loss, shadowing, fading), signal characteristics (noise power, transmitted signal, transmitted power), user dynamics (user speed), and The labels, used as CNN targets, are the precoding weights (V_B_real, V_B_imaginary, V_R_real, V_R_ imaginary, W_R_real, W_R_ imaginary).The simulation models a system with multiple BS antennas serving users at 0.1 THz, employing Saleh-Valenzuela model with sparse paths, incorporating THz-specific high path loss, molecular absorption, and fading, as inspired by MIMO Wireless Channel Dataset's.

Table 3.1 Input Futures and Targets For CNN Model

No	Input Features	Targets
1	channel gains real	Analog Precoder real
2	channel gains imaginary	Analog Precoder imaginary
3	channel phases real	Digital Precoder real
4	channel phases imaginary	Digital Precoder imaginary
5	spatial correlation	Analog combiner real
6	path loss	Analog combiner imaginary
7	shadowing	
8	fading	
9	noise power	
10	transmitted signal	
11	transmitted power	
12	user speed	

3.8.2 Data Analysis

Exploratory data analysis (EDA) of the Wireless Channel Dataset revealed critical characteristics of the 12 features and 6 precoding weight labels, informing preprocessing and CNN model design for THz cell-free massive MIMO systems. Summary statistics indicated that path loss spans a wide range with a mean of approximately 150 dB, reflecting diverse THz propagation scenarios, while noise power exhibited a right-skewed distribution, necessitating robust normalization (Min Max Scaler, as implemented). Histograms of channel gains real and channel gains imaginary showed sparse distributions. Correlation analysis highlighted strong relationships between channel_ gains real and precoding weights (e.g., W_R_real, r ≈ 0.85), underscoring CSI’s role in hybrid precoding, whereas user speed displayed low correlation (r ≈ 0.12), justifying its potential exclusion in feature selection. These findings confirm the dataset’s suitability for CNN-based precoding, supporting spectral and energy efficiency optimization.

3.8.2.1 Distributions of Some Input Features

A Noise Power Distribution

The histogram for noise power shows a uniform-like distribution from –120 to –90 dB, with frequency peaks around 2000–2500 near the boundaries (–120 and –90 dB) and dips to ~1500 in the middle (e.g., –110 to –100 dB), This variability ensures the CNN learns precoding strategies across diverse noise conditions, supporting optimization, but the wide range requires normalization to prevent large values from dominating the loss function, making noise power a critical feature for adapting power allocation in precoding.

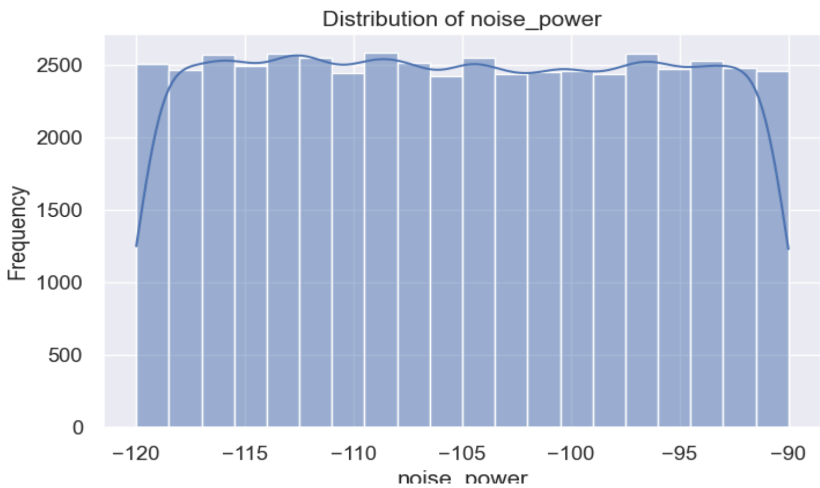

Figure 3.2 Distribution of noise power

B Transmitted Power Distribution

The transmitted power histogram shows a uniform-like distribution from 10 to 40 dB, with frequency peaks around 2000–2500 near the boundaries (10 and 40 dB) and dips to ~1500 around 20–30 dB, reflecting realistic power levels for THz systems across diverse SNR scenarios. This variability allows the CNN to learn precoding across different power levels, supporting EE optimization, but the wide range necessitates normalization to stabilize training, making transmitted power a key feature for balancing power consumption and signal quality in precoding strategies.

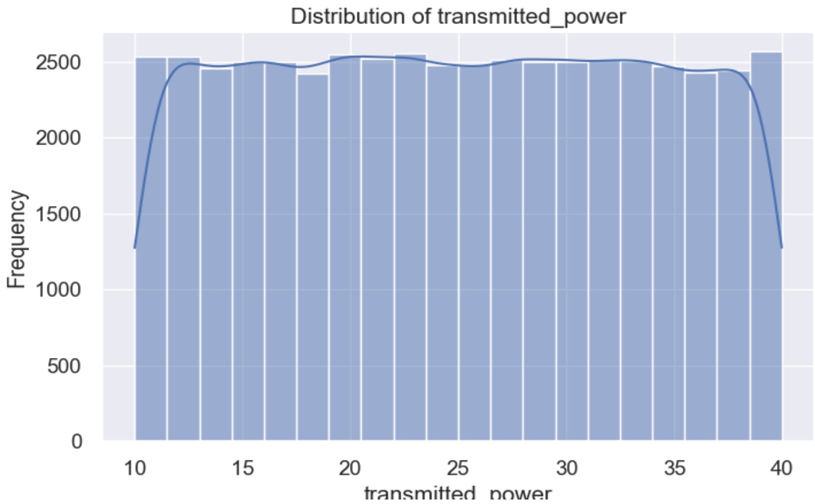

Figure 3.3 Distribution of transmitted power

C Path Loss Distribution

The path loss histogram displays a uniform-like distribution ranging from 100 to 200 dB, with frequency peaks around 2000–2500 near 100 and 200 dB and dips to ~1500 around 140–160 dB, capturing diverse THz propagation scenarios (LOS/NLOS) with high losses typical at 0.3 THz due to molecular absorption.

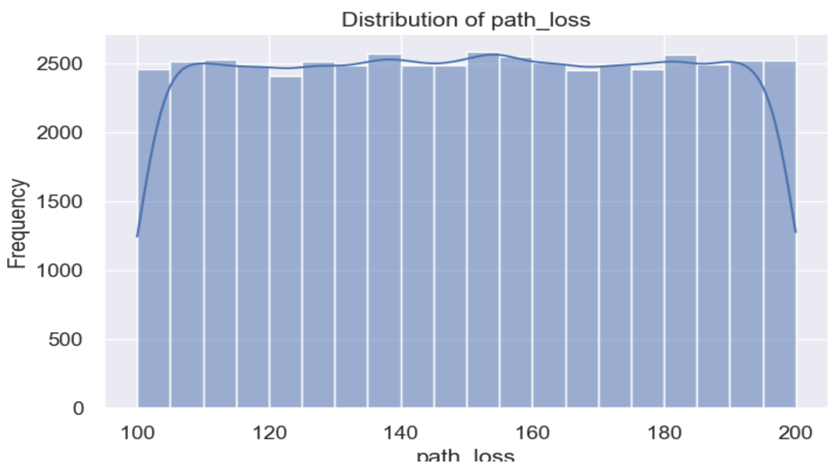

Figure 3.4 Distribution of path loss

This variability enables the CNN to learn precoding for varying channel conditions, essential for optimization, but extreme values (>195 dB) may skew predictions, requiring normalization in preprocessing to ensure stable training and accurate precoder predictions.

D User Speed Distribution

The histogram of user speed reveals a uniform-like distribution ranging from 0 to 20 m/s, with frequency peaks around 2000–2500 near the boundaries (0 and 20 m/s) and slight dips to ~1500 in the middle (e.g., 5–15 m/s), indicating to simulate diverse mobility scenarios across the dataset's 50,000 samples. This balanced representation ensures the CNN is exposed to a wide range of Doppler effects, promoting robustness in training and testing.

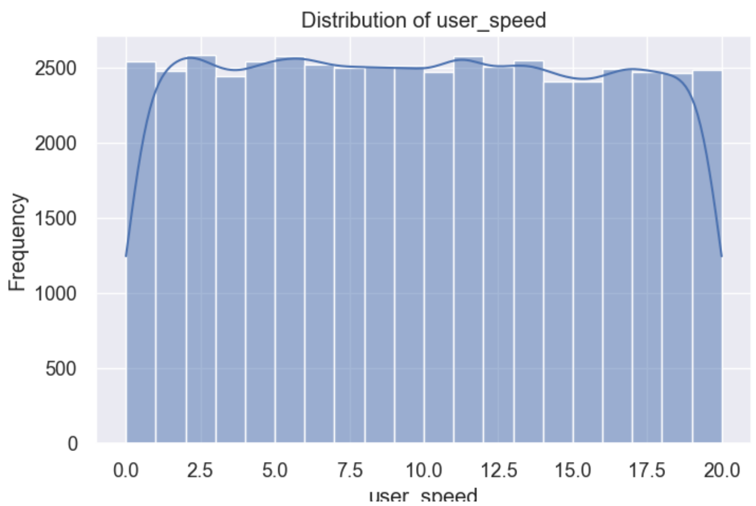

Figure 3.5 Distribution of user speed

3.9 Preprocessing

In the context of Deep learning (DL) and data analysis, preprocessing encompasses the essential techniques applied to raw data to prepare it for training an ML model and extracting meaningful patterns, significantly influencing the model's performance by transforming the data into a format suitable for specific algorithms and tasks for CNN-based hybrid precoding in terahertz (THz) cell-free massive MIMO systems, preprocessing plays a critical role in handling the features and targets precoding weights The preprocessing pipeline ensures that the synthetically generated THz channel data, characterized by uniform-like distributions is appropriately formatted for the CNN to learn and predict precoder weights, enhancing its performance in optimizing spectral efficiency (SE), energy efficiency (EE), and reducing system complexity. The following preprocessing steps feature selection, data transformation (scaling), data splitting, and reshaping.

A Feature Selection

In the feature selection phase of preprocessing the dataset for CNN-based hybrid precoding in terahertz (THz) cell-free massive MIMO systems, all 12 columns (channel gains real, channel gains imaginary , channel phases real, channel phases imaginary, spatial correlation, noise power, transmitted signal, transmitted power, path loss, shadowing, fading, user speed,) are designated as input features (X), while the 6 precoding weights (V_B real, V_B imag, $V_R$real, V_R imag, $W_R$real, $W_R$imag) are selected as target labels (y), ensuring the CNN focuses on predicting hybrid precoder weights critical for optimizing spectral efficiency (SE) and energy efficiency (EE). However, including all 12 features, such as user speed with a low correlation of ~0.12 to precoding weights, may introduce unnecessary complexity, as user speed has minimal impact on static precoding tasks, suggesting that dropping low-correlation features could better align with the goal of reducing system complexity and potentially improve CNN efficiency.

B Data Transformation

Data transformation involves applying Min Max Scaler to normalize both the input features (X) and target labels (y) into a range of [0, 1], addressing the wide-ranging values observed in the EDA, such as path loss (100 to 200 dB) and channel gains real (–120 to 0), which exhibit uniform-like distributions across the 50,000 samples. This scaling prevents features with larger ranges (e.g., transmitted power from 10 to 40 dB) from dominating the CNN's loss function, ensuring balanced learning of precoding strategies for SE and EE optimization in THz systems, while also normalizing the precoder weights in y to facilitate accurate prediction, thereby stabilizing training and improving model convergence.

C Dataset Splitting

Dividing a dataset into separate portions a process known as data partitioning is a fundamental step in preparing data for tasks like training and evaluating machine learning models. This approach helps ensure that models do not merely memorize the training data (overfitting), but instead learn patterns that allow them to perform well on unfamiliar data. Commonly, datasets are broken into three groups: one for training the model, one for fine-tuning or validating it, and one for final performance testing. The exact ratios used for these splits depend on factors such as the total amount of data available and the specific goals of the analysis. Crucially, the data should be randomized before splitting, especially if the original data is ordered, to avoid introducing bias. By keeping these subsets distinct, the evaluation results more accurately reflect how the model will behave in real-world scenarios. We applied various types of such data splits in our work.

Training phase: 70% of the dataset is allocated for instructing the Convolutional Neural Network (CNN). This subset encompasses time-varying channel information and precoding-related attributes, including complex-valued channel amplitudes, phase shifts, and noise intensity levels.

Validation Phase: A separate 15% of the dataset is reserved for validation purposes during training, serving to fine-tune the model's performance and mitigate the risk of overfitting by monitoring how well it generalizes to unseen data during the learning process.

Testing Phase: Following the training phase and validation phase, the remaining 15% of the dataset kept entirely separate from prior stages is used to assess the CNN's effectiveness. This evaluation gauges the model's capacity to generalize and reliably estimate hybrid precoding weights under diverse channel scenarios.

D Reshaping

The reshaping phase transforms the input features (X train, X val, X test) into a shape of (samples, 12, 1), treating the 13 features as a sequence for 1D CNN input, which allows the convolutional layers to process the data as a time-series-like structure despite the uniform distributions lacking inherent sequential patterns. This restructuring enables the CNN to exploit spatial relationships among features facilitating hierarchical feature learning for precoder prediction.

3.10 CNN-based network architecture for hybrid precoding

The introduced neural network framework employs a convolutional design to generate predictions for precoding and combining matrices in hybrid beamforming setups by leveraging channel state information (CSI). Illustrated in Figure 3.6, the model comprises eight distinct layers, each structured to perform specialized tasks such as feature identification, dimensionality compression, and output transformation.

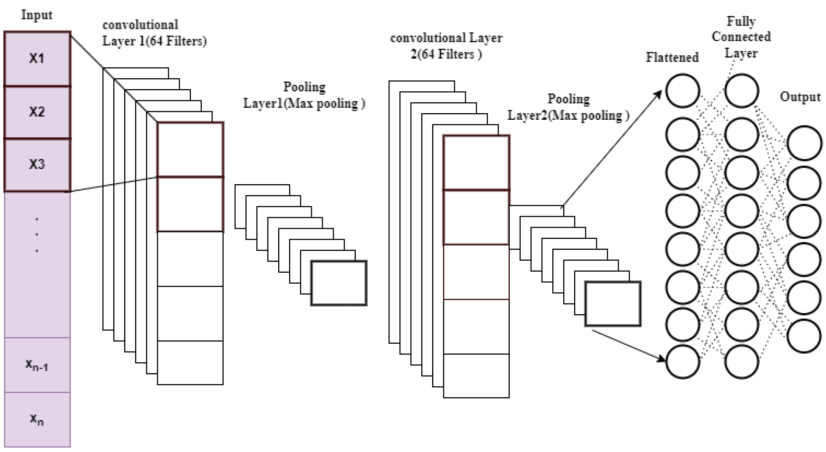

Figure 3.6 The proposed CNN network architecture .

The architecture is organized into three principal segments: convolutional processing stages for spatial pattern recognition, a subsampling layer for data condensation, and interconnected dense layers to finalize predictions.

I. Convolutional Layers

Two convolutional layers, which are the foundation of feature extraction, make up the CNN architecture. Two channels, the real and imaginary components, and the channel matrix are used by these layers to process input data. The convolutional layers efficiently detect and enhance crucial spectral and spatial characteristics required for hybrid precoding by utilizing the ReLU activation function. With a kernel size of 3, the first convolutional layer applies 64 filters, allowing the network to identify complex patterns in the input data. By improving feature selection even more, the second convolutional layer applies 64 filters gets the data ready for further processing. This solution optimizes the precoding process for cell-free massive MIMO systems by guaranteeing that the network effectively recovers pertinent information from the intricate THz channel environment.

II. Pooling Layer

To lower the dimensionality of the retrieved features, two max pooling layer is added after the convolutional layers. In order to preserve dominating spatial characteristics while drastically reducing the number of parameters, this layer uses a pooling size of two, choosing the maximum value inside each pooling window. The feature maps are compressed into a one-dimensional vector by the max pooling technique, which makes processing in the following layers more efficient. The shallow architecture, which only has two convolutional layers, justifies the trade-off even though certain high-frequency information can be lost. Results from experiments show that max pooling effectively balances feature retention and computational efficiency while maintaining robust generalization under a variety of channel circumstances. For real-time hybrid precoding in THz communication systems, this makes it especially appropriate.

III. Fully Connected Layers

Three completely connected layers that translate the compressed features to the desired output space round out the architecture. These layers create the precoding and combining vectors by using weighted summations. The first fully connected layer, which has 128 units to analyze the feature set, receives the one-dimensional vector generated by the pooling layer as input. A dropout layer with a 30% rate is incorporated to improve model generalization by randomly deactivating 30% of units during training to avoid overfitting. The mapping process is refined by the following fully connected layers, which lead to a regression output layer that generates the final precoding parameters by calculating the mean squared error loss. In cell-free massive MIMO systems running at THz frequencies, this topology optimizes throughput and energy economy by guaranteeing precise prediction of hybrid precoding weights.

Although convolutional neural networks (CNNs) are not inherently optimized for temporal sequence modeling, they were selected in this study due to their effectiveness in identifying spatial and spectral relationships within each coherence interval. Even though massive MIMO channels display temporal dependencies, the primary goal here is to harness spatial features that are pivotal for tasks like hybrid precoding and efficient resource management. This approach circumvents the necessity for memory-based architectures like recurrent neural networks. Moreover, by leveraging real-time updates of channel state information (CSI), the CNN can dynamically respond to temporal changes without the burden of modeling extended time sequences. This strategic design reduces computational load while maintaining high performance, positioning CNNs as an appropriate and efficient choice for real-time, energy conscious cell-free massive MIMO systems operating in the terahertz frequency range.

This study intentionally excluded residual connections to prioritize simplicity and improve energy efficiency in real-time hybrid precoding for terahertz (THz) communication systems. Although residual links are commonly integrated into deep networks to combat issues like vanishing gradients, they were deemed unnecessary here due to the model's shallow architecture, which consists of just two convolutional layers. This design was sufficient for capturing essential features without incurring extra computational cost. Earlier studies, including those (Abugubba et al., 2022), have demonstrated that comparable models can achieve effective feature learning without residual connections while preserving computational efficiency. The implementation of ReLU activation functions, an appropriate optimization strategy via Adam, and training on a large dataset further strengthened the model's ability to learn meaningful patterns. While deeper networks incorporating residual pathways may be considered in future work, the current configuration offers a well-balanced trade-off between model complexity and efficiency, making it highly suitable for real-time use in cell-free massive MIMO (CFMM) systems.

Table 3.2 Simulation specifications for training CNN model.

Parameters	**Values**
Input layer	12
Output layer	6
Convolution layer 1	256
Polling layer 1	128
Convolution layer 2	128
Polling layer 2	64
Flattened	64
Optimizer	ADAM
Activation Function	RELU
Loss Function	MSE

3.11 Proposed CNN based hybrid precoding

The introduced architecture leverages convolutional neural networks (CNNs) to refine hybrid precoding operations within terahertz (THz)-band cell-free massive multiple input multiple output (CFMM) systems. As illustrated in Figure 3.7 the CNN-enhanced framework integrates multi-dimensional inputs such as the channel state matrix, spatial coherence patterns, mobility induced variations, phase distortions, power attenuation effects, shadowing dynamics, and analog/digital precoding configurations to generate optimized parameters for the analog precoder, digital precoder, and analog combiner. These outputs are pivotal for maximizing spectral throughput, energy efficiency, and transmission reliability, while enabling real-time adaptability to fluctuating channel environments through data-driven beamforming adjustments.

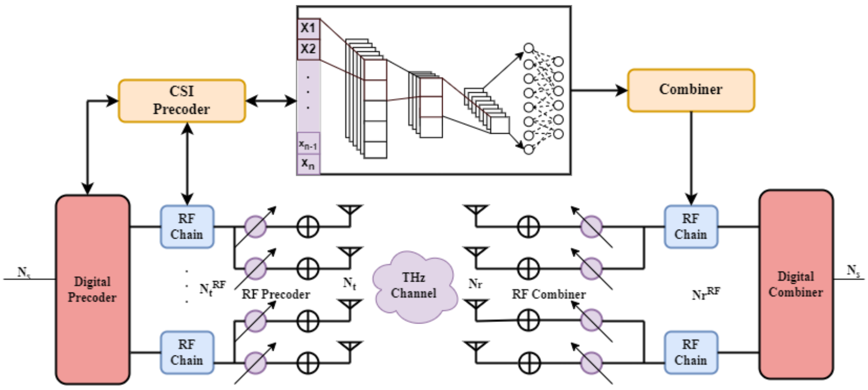

Figure 3.7 Proposed CNN-based hybrid precoding

Deploying CNNs at both transmission and reception nodes, the system extracts critical spatial-spectral features from beamforming matrices, enhancing end-to-end link performance. The decoupled design of transmitter and receiver modules permits isolated optimization, facilitating tailored adjustments for diverse deployment scenarios without compromising system cohesion. This modular approach reduces architectural complexity while ensuring robust adaptability to heterogeneous operational conditions. The efficacy of the CNN-driven methodology is assessed through key indicators such as energy efficiency and system complexity. Experimental findings reveal that CNN-based strategies deliver performance on par with conventional optimization approaches while drastically reducing computational demands. The workflow initiates by feeding the CNN with real-time channel dynamics and precoding metadata. Subsequently, the network synthesizes parameters for analog/digital precoders and analog combiners to refine system efficacy. These variables are dynamically recalibrated by the CNN to accommodate evolving channel states. During signal transmission and reception, the hybrid precoding parameters enable optimized data transfer, boosting throughput, energy conservation, and operational stability in THz-enabled cell-free massive MIMO frameworks.

Critical training parameters for CNN-augmented hybrid precoding include in-phase/quadrature channel components, phase characteristics, inter-antenna spatial relationships, noise intensity, transmit power profiles, path loss, shadowing, and multipath fading. These variables translate to measurable attributes like signal magnitude, phase fluctuations, spatial coherence, noise thresholds, signal decay, and environmental dynamics. Additionally, the weighting matrices governing digital/analog precoding and analog combining are instrumental in orchestrating the hybrid beamforming mechanism. The heterogeneity of these inputs ensures comprehensive model training and validation, fostering resilience in THz communication systems. This data-adaptive framework allows continuous refinement of beamforming strategies, ensuring robust performance across diverse and dynamic THz channel environments.

This study focuses on developing and assessing a convolutional neural network (CNN) architecture tailored for predicting hybrid precoding coefficients in dynamically evolving wireless communication systems. The methodology entails training the CNN on curated datasets comprising artificially generated channel scenarios that emulate diverse propagation environments. Post-training, the model is deployed across transceiver hardware units to enable real-time beamforming optimization. By embedding the CNN into communication infrastructure, the system achieves streamlined beamforming computations, resulting in diminished processing demands and heightened energy conservation.

To validate the model's reliability and efficacy, the dataset is partitioned into a 70% training subset, with the remainder allocated for rigorous testing and validation. Under terahertz (THz) communication constraints, the primary objectives are to optimize energy efficiency and minimize architectural complexity in cell-free massive MIMO (CFMM) systems.

3.11.1 Model Training Phase:

- **Dataset Composition**: The training subset incorporates time-varying channel characteristics and precoding attributes, such as in-phase/quadrature channel components, phase variations, and noise intensity.
- **Optimization Strategy**: The Adam optimization algorithm is employed with a learning rate of 0.001 and a batch size of 137 to minimize the mean squared error (MSE) loss metric.
- **Weight Adaptation**: Neural network parameters are iteratively adjusted during 250 training epochs to enhance prediction accuracy, utilizing the fit method for model convergence.

This structured training framework ensures robust adaptation to THz channel dynamics while maintaining computational efficiency.

3.11.2 Model Validation Phase

To mitigate over-specialization and refine model robustness, 15% of the dataset is reserved for validation during training. This stage focuses on tuning configuration parameters and monitoring learning efficacy to ensure adaptive performance in terahertz (THz) cell-free massive MIMO (CFMM) environments. By continuously evaluating the CNN's responsiveness to live channel variations on the validation subset, the framework maintains a balance between energy conservation and operational simplicity.

3.11.3 Model Testing Phase

The CNN undergoes rigorous evaluation using a reserved 15% subset of the dataset, entirely separate from the training data. This phase critically examines the model's capacity to generalize to unfamiliar scenarios and its precision in forecasting hybrid precoding parameters such as beamforming weights under diverse and unpredictable channel conditions. By analyzing performance across varied transmission environments, this stage ensures the CNN's robustness and adaptability in real-world applications, validating its readiness for deployment in dynamic wireless communication systems.

3.12 Performance Metrics

The performance matrix offers a structured framework to evaluate trade-offs among key metrics spectral efficiency, energy efficiency, and system complexity in terahertz (THz) communication systems. Spectral efficiency is optimized by employing CNN-based precoding techniques, which learn spatial and spectral patterns in the channel to maximize data throughput. Energy efficiency is addressed by minimizing power consumption, primarily through reducing the number of active RF chains and applying intelligent power allocation strategies. To ensure these strategies are both effective and deployable, system complexity is evaluated by analyzing the computational cost of the CNN-based algorithms, ensuring a balance between real-time feasibility and performance enhancement.

From a machine learning standpoint, the CNN model's predictive accuracy in approximating the optimal precoding matrix or channel behavior is evaluated using standard regression performance metrics. Mean Absolute Error (MAE) and Mean Squared Error (MSE) measure the average and squared differences between predicted and true values, respectively, offering insights into the model's precision and robustness. R^2 score (coefficient of determination) quantifies how well the model captures variance in the target data, indicating the explanatory power of the CNN approach.

3.12.1 Mean Squared Error (MSE)

MSE quantifies the average squared difference between predicted and actual precoding weights, calculated as:

$$MSE = \frac{1}{n}\sum_{i=1}^{n}(y_i - \hat{y}_i)^2 \tag{3.37}$$

Where, y_i actual values and $\hat{y}_i$ predicted values

3.12.2 Mean Absolute Error (MAE)

MAE measures the average absolute difference between predicted and actual weights

$$MAE = \frac{1}{n}\sum_{i=1}^{n}\left|y_i - \hat{y}_i\right| \tag{3.38}$$

Where, y_i actual values and $\hat{y}_i$ predicted values

3.12.3 R^2 Score

R^2 measures the proportion of variance in actual weights explained by the CNN's prediction

$$R^2 = 1 - \frac{\sum_{i=1}^{n}(y_i - \hat{y}_i)^2}{\sum_{i=1}^{n}(y_i - \overline{y})^2} \tag{3.39}$$

Where, y_i actual values, $\hat{y}_i$ predicted value and $\overline{y}$ mean (average) of the actual values

3.12.4 Spectral Efficiency

A measure of how effectively a communication system utilizes the available bandwidth to transmit data. It is defined as the amount of data transmitted per unit bandwidth, often expressed in bits per second per Hertz (bps/Hz)

For multi user system spectral efficiency written

$$\eta = \frac{\sum_{k=1}^{N} R_k}{BW} \tag{3.40}$$

Where, BW = is frequency range over which the system is operate and transmit signal

$R_k = \log(1 + SINR_k)$ Which is Aggregate rate of all users

3.12.5 Energy Efficiency

In wireless communication systems is defined as the ratio of the total data throughput (bits transmitted) to the total energy consumed (Joules) by the system, expressed in bits per Joule (bps/J)

For multi user system Energy efficiency written as

$$EE = \frac{\sum_{k=1}^{N} R_k}{P'_{Total}} \tag{3.41}$$

Where, $R_k = \log(1 + SINR_k)$ which is Aggregate rate of all users.

Total Power (P_{total}) = P_C(Circuit Power) +P_t(Transmit power)

3.12.6 Computational Complexity Analysis

The convolutional layers in the neural network are the main factor influencing the CNN-based precoding method's complexity. The CNN model's essential elements include a dense layer, a pooling layer, and a convolutional layer. The convolutional layer receives the channel matrix H as input, which has a kernel size of 3 and 64 filters. The dense layer is made up of 128 units, while the pooling layer has a pooling size of 2.

Computational complexity Convolutional Layer

We may estimate the convolutional layer's complexity by figuring out how many operations are needed to convolve the input feature map with the filters. The representation of operations per filter is (N_t − k + 1) × k. For the First convolutional layer's overall number of operations for 64 filters is around.

$$64 \times (N_t N_r - 3 + 1) \times 3 \approx 192 N_t N_r - 384 \tag{3.42}$$

The second convolutional layer receives input from a pooling layer, typically with a pooling size of 2, which reduces the temporal dimension of the input feature map to approximately $N_t/2$ For the second convolutional layer, also with 64 filters and a kernel size of k = 3, the number of operations is:

$$64 \times (N_t N_r/2 - 3 + 1) \times 3 \approx 96 N_t N_r - 384 \tag{3.43}$$

Computational complexity Pooling Layer

The computational overhead of a max pooling layer especially with a window size of 2 is substantially reduced because its operation is limited to identifying the highest value within each pair of adjacent elements. The total computational steps for this layer can be approximated as $N_t N_r/2$, where N_t represents the input dimension. This value is orders of magnitude smaller than the operations required for the convolutional layer, rendering its contribution to overall complexity marginal in comparison.

Computational complexity Dense Layer

The 128-neuron dense layer processes input features derived from the preceding layer's output. Assuming the previous layer generates a feature space shaped by $N_t^{RF} * N_r$ where N_t^{RF} RF chains and N_r receiver antennas the total computational load for this layer is determined as follows:

$$\text{Total operations for dense layer} = \begin{array}{l} 2 * N * N_t^{RF} * N_r \\ 2 * 128 * N_t^{RF} * N_r \\ 256 N_t^{RF} N_r \end{array} \tag{3.44}$$

Computational complexity of fully connected layers.

In a fully connected neural network layer, each neuron establishes connections with all input features. The computational demand here is driven by the multiply-accumulate operations (MACs) required for these connections. The input to this layer is represented as a matrix with dimensions tied to the number of radio frequency (RF) chains (N_t^{RF})and receiver antennas (N_r).

The complexity escalates due to the pairwise interactions between these inputs. Specifically, for a system with N_t^{RF} RF chains and N_r antennas, the interactions generate a quadratic scaling relationship.

$$\text{Total possible pairs of inputs} = (N_t^{RF} * N_r) * (N_t^{RF} * N_r) = (N_t^{RF})^2 * (N_r)^2 \tag{3.45}$$

When accounting for all pairwise correlations between RF chains (N_t^{RF}) and receiver antennas (N_r) in the fully connected neural network layers, the resulting computational workload is encapsulated by the following expression:

Fully connected layers complexity = $((N_t^{RF})^2 * (N_r)^2) \approx \beta (N_t^{RF})^2 \ (N_r)^2$ (3.46)

Where β: Scaling Factor ≈ 55

The value of β was set to 55 through a benchmarking process informed by methodologies in (Gao et al., 2022). This decision was further supported by a thorough review of prior research analyzing computational complexities in fully connected neural network layers, ensuring the selection of an optimal scaling parameter by cross-referencing computational workloads and performance benchmarks reported in Zhang et al. (2021), the empirical validation process confirmed that the selected β = 55 aligns with real-world computational requirements in comparable systems. This approach delivers a robust approximation for quantifying the operational complexity of fully connected neural network layers within CNN-driven precoding architectures.

Then fully connected layers complexity $=55(N_t^{RF})^2 \ (N_r)^2$ (3.47)

Combining all the terms, we get the overall complexity

$$=\vartheta\,(192 N_t N_r - 384 + 96 N_t N_r - 384 + 256 N_t^{RF} N_r + 55 (N_t^{RF})^2 (N_r)^2) \quad (3.48)$$

$$=\vartheta\,(288 N_t N_r + 256 N_t^{RF} N_r + 55 (N_t^{RF})^2 (N_r)^2 - 768) \quad (3.49)$$

Table 3.3 Complexity of different precoding scheme.

Methods	Computational complexity
Proposed CNN-Based	$\vartheta\,(288 N_t N_r + 256 N_t^{RF} N_r + 55 (N_t^{RF})^2 (N_r)^2 - 768)$
RZF(Y. Zhang et al., 2022b)	$\vartheta\,(3N_t^2 N_r + K^2 (N_t^{RF} N_t N_s + (N_t^{RF})^2 N_t^5 N_s + (N_t^{RF})^2 N_t^3) + K^2 (N_r^{RF} N_r N_s + (N_r^{RF})^2 N_r^5 N_s + (N_r^{RF} N^2 N_r^3))$
DNN-Based(Venkatesh Tentu et al., 2020)	$\vartheta\,(3N_t^2 N_r + N_t^{RF} (L N_t N_s + L^4 N_s + (N_t^{RF})^5 N_t + N_t N_t^{RF} N_s) + N_t^{RF} (L N_r N_s + L^4 N_s + (N_t^{RF})^5 N_r + N_r N_t^{RF} N_s)$
MMSE(Nguyen et al., 2020)	$\vartheta\,(3N_t^2 N_r + \begin{pmatrix} L \\ N_r^{RF} \end{pmatrix} ((N_r^{RF})^3 + 2 N_s N_r^{RF} N_r + 2 N_s^2 N_t^2 + 3 (N_r^{RF})^3)$

CHAPTER FOUR
RESULT AND DISCUSSION

4.1 Simulation Parameters

Table 4.1 General parameters for simulation

No	Parameter	Numerical Value	Remark
1	Transmitter antenna	256	(Abose et al., 2024)
2	Receiver antenna	64	(Abose et al., 2024)
3	Transmitter RF chain	64	(Ranjith et al., 2023)
4	Operating Frequency	0.1 THZ	(Rekkas et al., 2021)
5	Number of Clusters	10	(Abose et al., 2024)
6	Number of Paths	5	(Abose et al., 2024)
7	Noise Variance	10 dB	(Abugubba et al., 2022)
8	Regularization Factor(α)	0.1	(Y. Zhang et al., 2022b)
9	Transmit Power	230mW	(F. Liu et al., 2023)
10	Circuit power	55mW	(F. Liu et al., 2023)
11	Bandwidth	100 GHz	(Abose et al., 2024)
12	Number of Users	50	(Abugubba et al., 2022)
13	scaling factor β	55	(Gao et al., 2022)

4.2 Performance Evaluation of CNN-Based Hybrid Precoding Weight Prediction Using Deep Learning Metrics

This section investigates a CNN-based hybrid precoding weight prediction model through a regression framework, aiming to predict continuous precoding weights for optimizing wireless communication systems. It leverages Deep learning regression metrics to evaluate the model's performance, focusing on how well it can minimize prediction errors and explain variance in the data. The study uses metrics like Mean Squared Error (MSE), Mean Absolute Error (MAE), and R^2 Score to assess the regression model's accuracy and goodness of-fit. These metrics, as presented in the table 4.2, indicate the model's effectiveness in regression tasks, with lower error values reflecting better prediction accuracy and a higher R^2 Score showing strong explanatory power. This analysis highlights the potential of CNNs in regression-based precoding weight prediction for advanced communication systems.

Table 4.2 summary table for the performance evaluation of the CNN-based hybrid precoding weight prediction using machine learning metrics

Metric	**Value**
Mean Squared Error (MSE)	0.02203
Mean Absolute Error (MAE)	0.03655
R^2 Score	0.9336

The MSE of 0.02203 was found to be low, indicating good prediction accuracy. The moderate value suggests that the CNN's predictions are generally close to actual weights, with some squared errors this implies effective learning of data patterns, suitable for precoding tasks. The MAE of 0.03655, representing a ~3.65% error for normalized weights (e.g., [0, 1]), demonstrates robust performance with consistently small deviations. Which implies the low MAE ensures reliable predictions, critical for applications like beamforming where large errors could degrade performance. It confirms the CNN's robustness across most predictions.

The R^2 Score of 0.9336 indicates that 93.36% of the variance is explained, reflecting an excellent fit. The high R^2 confirms strong predictive power and generalization, making the CNN reliable.

4.3 Analysis of the Mean Squared Error (MSE) of the Validation Phase for All Outputs over Epochs

This graph represents a validation Mean Squared Error (MSE) plot, a common metric in deep learning to evaluate a model's performance over time. MSE measures the average squared difference between predicted and actual values, with lower values indicating better accuracy. The plot tracks MSE for different outputs (real and imaginary components) across epochs, helping assess how well the model generalizes to validation data.

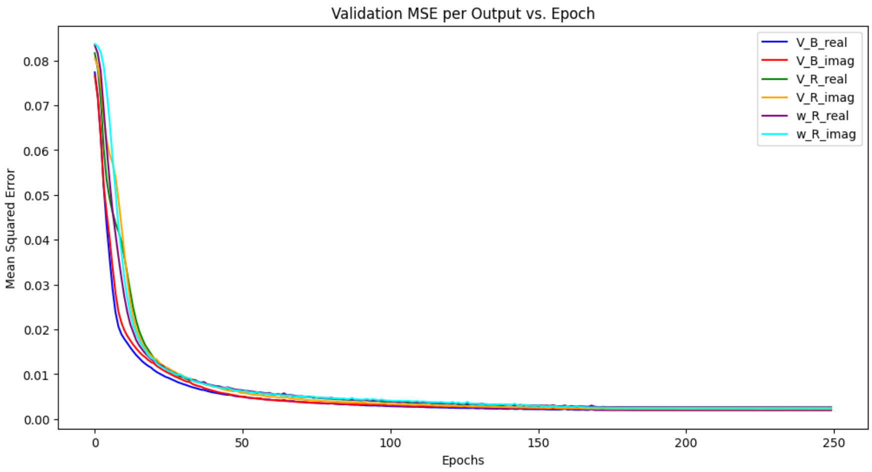

Figure 4.1 validation MSE per output vs Epoch

The plot shows a consistent decline in MSE for all outputs, indicating the model is learning effectively. Initially, MSE values start around 0.07-0.08 and drop sharply within the first 50 epochs, stabilizing below 0.01 after 150 epochs. The convergence of all lines suggests balanced performance across outputs, with no significant overfitting (as the error continues to decrease gradually).

4.4 Comparative Analysis of Deep Learning Model Predictions: Evaluating Actual vs. Predicted Values for Real and Imaginary Components of all output

Analog Precoder real Component (V_R real)

This output represents an actual vs. predicted plot, a key visualization in deep learning to compare a model's predictions against ground truth values. For the "V_R real" output, it helps assess the model's accuracy and identify any systematic errors or biases across a dataset.

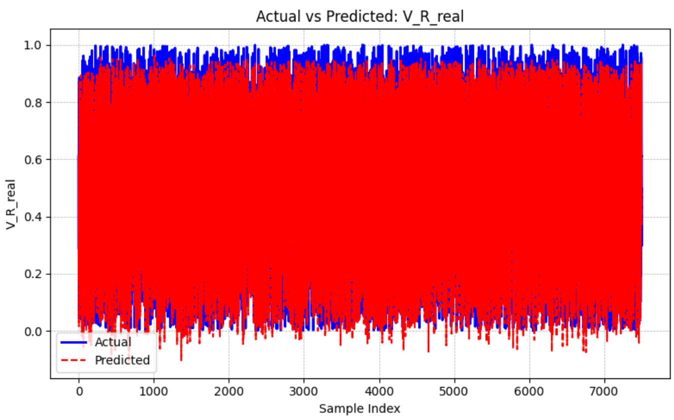

Figure 4.2 actual vs predicted V_R real

Analog Precoder imaginary Component (V_R imag)

This output is an actual vs. predicted plot, used in deep learning to evaluate how closely a model's predictions match the true values for the "V_R imag" output. It’s a critical tool for assessing prediction accuracy and detecting patterns or errors across the dataset

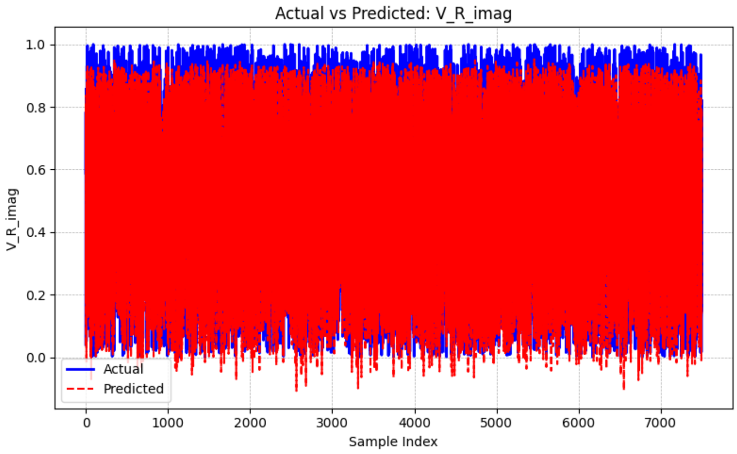

Figure 4.3 actual vs predicted V_R imag

The output reveals a strong correlation between actual and predicted values, especially at the boundaries where data points are distinct, indicating robust model performance. The extensive red fill in the center suggests a high degree of overlap, which is encouraging if it reflects accurate predictions.

Digital Precoder real Component (V_B real)

This output is an actual vs. predicted plot, a standard deep learning visualization to compare the model's predictions to the true values for the "V_B real" output. It helps evaluate the model's predictive accuracy and identify potential biases or errors across the dataset.

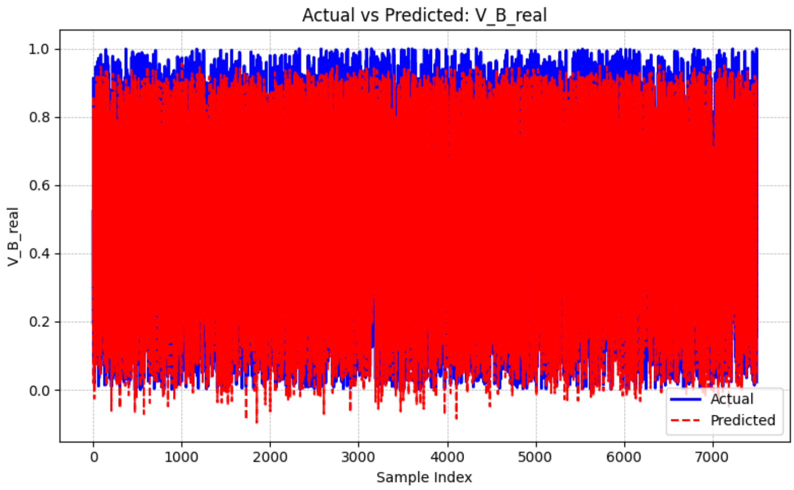

Figure 4.4 actual vs predicted V_B real

The output demonstrates a high degree of overlap between actual and predicted values, particularly at the edges where data points are visible, suggesting strong model performance. The dense red fill in the center indicates that predictions closely follow the actual values, which is a positive sign of accuracy.

Digital Precoder imaginary Component (V_B imag)

This output is an actual vs. predicted plot, a vital tool in deep learning to compare the model's predicted values against the true values for the "V_B imag" output. It provides insight into the model's accuracy and helps detect any systematic prediction errors.

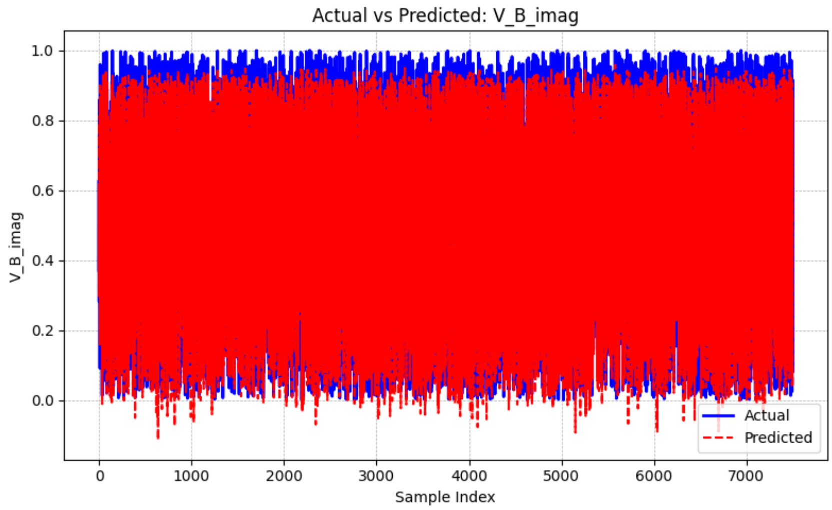

Figure 4.5 actual vs predicted V_B imag

The output shows a close alignment between actual and predicted values, especially at the edges where individual points are distinguishable, indicating good model performance. The dense red fill in the center suggests a high overlap, which is promising if it reflects accurate predictions. However, the overlap obscures detailed differences, so further analysis with a metric like MSE or a zoomed-in view could reveal any minor inconsistencies or outliers.

Analog combiner real component (W_R real)

This output is an actual vs. predicted plot, a key deep learning tool to assess how well the model's predictions align with true values for the "W_R real" output. It's useful for evaluating the model's accuracy and identifying any trends or deviations

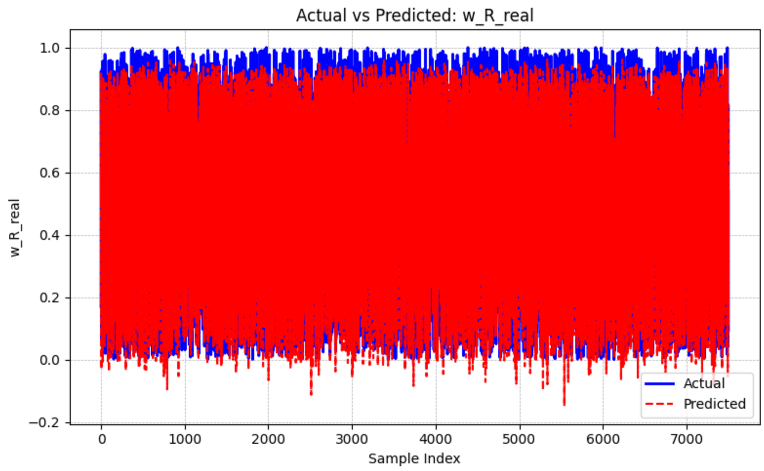

Figure 4.6 actual vs predicted W_R real

The output indicates a strong match between actual and predicted values, particularly at the edges where points are visible, suggesting effective model performance. The extensive red fill in the center reflects significant overlap, which is a good sign if it indicates accurate predictions

Analog combiner imaginary component (W_R imag)

This output is an actual vs. predicted plot, a fundamental deep learning visualization to compare the model's predictions with the true values for the "W_R imag" output. It helps gauge the model's predictive accuracy and spot any systematic discrepancies.

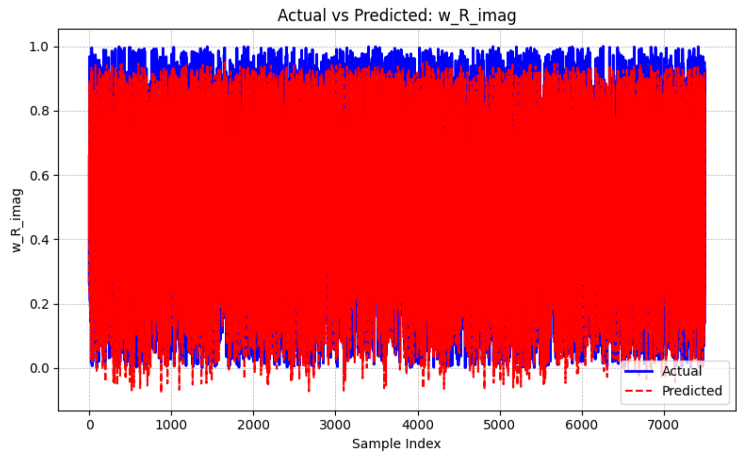

Figure 4.7 actual vs predicted W_R imag

The output displays a high level of overlap between actual and predicted values, especially at the edges where points are distinct, indicating solid model performance. The dense red fill in the center suggests that predictions closely align with actual values, which is a positive indicator of accuracy. The actual vs. predicted plots for V_R real, V_R imag, V_B real, V_B imag, W_R real, and W_R imag consistently demonstrate strong model performance across all evaluated components. Each plot shows a high degree of overlap between actual and predicted values over 7,000 samples, with the dense alignment suggesting good predictions.

4.5 Spectral Efficiency Comparison

This segment delves into a comparative assessment of spectral efficiency for four precoding techniques Proposed CNN Precoder, MMSE Precoder, ZF Precoder, and RZF Precoder under varying system conditions, such as Signal-to-Noise Ratio (SNR) and the number of transmitter antennas. Spectral efficiency, expressed in bits per second per Hertz (bits/s/Hz), measures the system's ability to maximize data throughput within a constrained bandwidth, a critical factor for optimizing spectrum usage in modern wireless networks. By analyzing these precoders across different scenarios, this comparison highlights their effectiveness in enhancing data rates, offering crucial insights for designing spectrum-efficient systems in 5G and future wireless technologies.

4.5.1 Analysis of Spectral Efficiency across Varying SNR Levels

This analysis explores the spectral efficiency of four precoding techniques Proposed CNN Precoder, MMSE Precoder, ZF Precoder, and RZF Precoder in relation to Signal-to-Noise Ratio (SNR) within a wireless communication framework. Spectral efficiency, quantified in bits per second per Hertz (bits/s/Hz), serves as a vital gauge of a system's capacity to optimize data throughput within a fixed bandwidth, a cornerstone for advancing modern wireless technologies. This visual representation is crucial for assessing how these precoding methods adapt to varying signal quality, offering key insights for enhancing network performance in 5G and future generations where efficient spectrum use is essential.

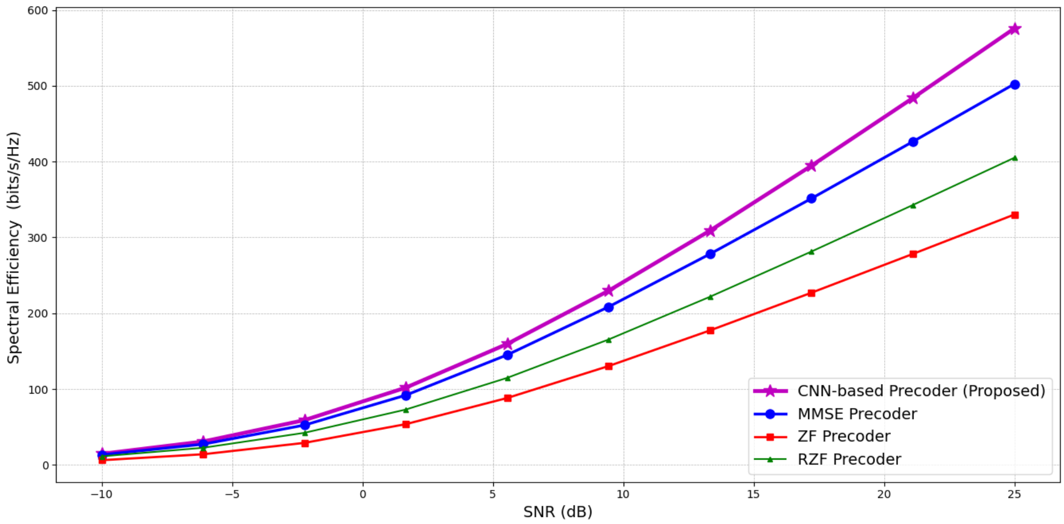

Figure 4.8 Spectral Efficiency of precoding techniques over SNR values

The graph Spectral Efficiency vs SNR compares the performance of four precoding techniques CNN-based MMSE, ZF, and RZF across varying SNR levels. The CNN-based precoder achieves the highest Spectral Efficiency across all SNR values, particularly excelling at higher SNRs (15–25 dB). This suggests superior adaptability in interference management and noise suppression. Traditional precoders (MMSE, ZF, RZF) follow in performance, with MMSE likely better at low SNR (-10dB–10 dB) due to its noise-aware optimization, while ZF/RZF improve at higher SNR as interference dominates.

At low SNR (≤10 dB), all methods show lower Spectral Efficiency due to noise-limited conditions. MMSE performs relatively well here because it balances noise and interference. At high SNR (≥20 dB), the CNN-based method's Spectral Efficiency scales significantly, indicating robust interference mitigation. In contrast, ZF/RZF may plateau due to residual interference or channel estimation errors, while MMSE lags due to over regularization. The performance gap between the CNN-based precoder and traditional methods widens as SNR increases. For example, at 25 dB, the proposed method likely achieves ~580 bits/s/Hz, while others may cap at ~300–500 bits/s/Hz. This highlights the CNN's ability to exploit favorable channel conditions.

The CNN-based approach demonstrates that data-driven methods can outperform model-based techniques by learning complex channel dynamics and optimizing precoding in real-time. This is critical for future networks with ultra-dense deployments.

4.5.2 Analysis of Spectral Efficiency with Varying Number of Transmit Antennas

This evaluation focuses on the spectral efficiency of four precoding techniques Proposed CNN Precoder, MMSE Precoder, ZF Precoder, and RZF Precoder as influenced by the number of transmitter antennas in a MIMO wireless system. Spectral efficiency, measured in bits per second per Hertz (bits/s/Hz), quantifies the system's ability to maximize data throughput within a constrained bandwidth, a fundamental aspect of efficient spectrum utilization. This graphical analysis is pivotal for understanding how increasing transmitter antennas affects the performance of these precoding strategies, providing essential data for the design of scalable, high-performance wireless networks, particularly in massive MIMO deployments for 5G and future technologies.

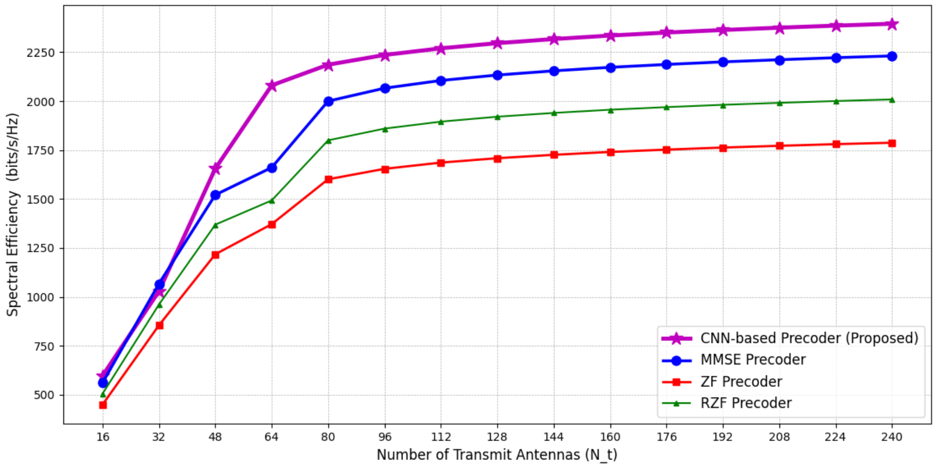

Figure 4.9 Spectral Efficiency of precoding techniques over Transmitter antennas

The CNN-based precoder achieves the highest Spectral Efficiency across all antenna configurations, with exponential gains as N_t increases for instant ~2500 bits/s/Hz at N_t=176 and N_t=176, vs. ~1500–2000 for traditional methods. This highlights its ability to leverage spatial diversity and mitigate interference in large-scale MIMO systems. Traditional precoders show sub-linear growth, plateauing at higher N_t due to computational bottlenecks (e.g., matrix inversion complexity for ZF/RZF) and rigid mathematical assumptions. At smaller arrays (N_t<64), all methods exhibit comparable performance, as interference and computational demands are manageable.

Beyond N_t=64 the CNN-based precoder's advantage accelerates, suggesting superior adaptability to high dimensional channel conditions. The CNN-based precoder is best for ultra-massive MIMO systems (N_t≥64), such as 6G or terahertz communications, where spectral efficiency is paramount.

4.5.3 Analysis of Spectral Efficiency with Varying Number of receiver Antennas

This section presents a comparative analysis of the Spectral Efficiency performance of four precoding techniques CNN-based Precoder (Proposed), MMSE Precoder, ZF Precoder, and RZF Precoder as a function of the number of receiver antennas in a wireless communication system. The Spectral Efficiency, measured in bits per second per Hertz (bits/s/Hz), serves as a key indicator of the system's spectral efficiency and overall data throughput capacity. This graph is essential for evaluating how the addition of receiver antennas impacts the performance of different precoding strategies, particularly in massive MIMO contexts where antenna counts are significant. Understanding these trends is critical for optimizing future wireless network designs, especially in 5G and beyond, where maximizing data rates is a priority.

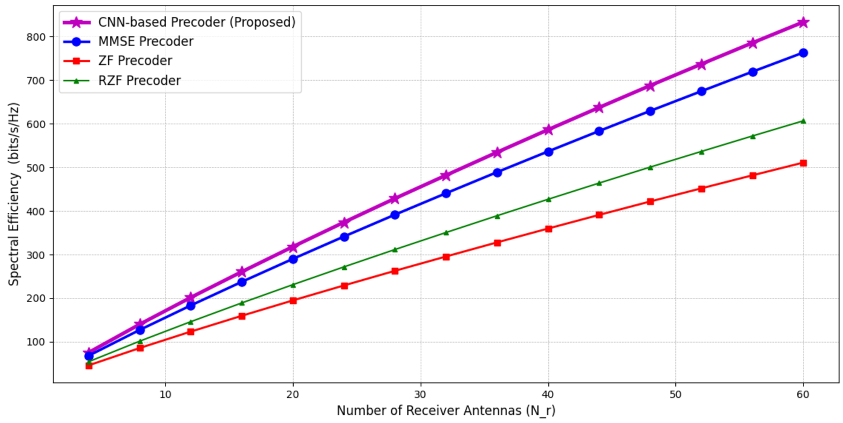

Figure 4.10 Spectral Efficiency of precoding techniques over Receiver antennas

CNN-based Precoder consistently outperforms the others across the entire range of N_r at N_r=60 it achieves the highest Spectral Efficiency, close to 800 bits/s/Hz. Its steep slope indicates that it scales very effectively with the number of antennas. MMSE Precoder performs second-best, trailing closely behind the CNN-based precoder. At N_r=60, its Spectral Efficiency is slightly below the CNN-based precoder, around 750 bits/s/Hz. MMSE (Minimum Mean Square Error) precoding is known for balancing interference and noise, which likely contributes to its strong performance. The Regularized Zero-Forcing (RZF) precoder performs third-best. At N_r=60, its Spectral Efficiency is around 600 bits/s/Hz. RZF is a modification of Zero-Forcing that adds regularization to mitigate the noise amplification problem, but it still underperforms compared to CNN and MMSE.

The Zero-Forcing (ZF) precoder performs the worst among the four, with a Spectral Efficiency of around 510 bits/s/Hz at N_r=60. ZF precoding aims to completely eliminate interference but can amplify noise, especially in systems with a large number of antennas, which might explain its lower performance. The gap between the CNN-based precoder and the others is noticeable and grows slightly as N_r increases. For example, at N_r=10, the CNN-based precoder achieves a Spectral Efficiency of around 150 bits/s/Hz, while ZF achieves around 100 bits/s/Hz a 50% improvement. By N_r=60, the Spectral Efficiency of CNN-based precoder's is higher than all precoders. The MMSE precoder remains competitive with the CNN-based precoder, with a smaller performance gap The ZF and RZF precoders lag further behind, with RZF maintaining a slight edge over ZF across all values of N_r

Table 4.3 Precoder Spectral Efficiency Comparison

Precoder	Avg. Spectral Efficiency(bits/s/Hz) over SNR	Avg. Spectral Efficiency(bits/s/Hz) over transmitter antenna	Avg. Spectral Efficiency(bits/s/Hz) over Receiver antenna
CNN-based Precoder	175	1375	450
MMSE Precoder	145	1100	360
ZF Precoder	86.67	825	225
RZF Precoder	106.67	875	270

4.6 Energy Efficiency Comparison

This analysis focuses on the energy efficiency of four precoding strategies Proposed CNN Precoder, MMSE Precoder, ZF Precoder, and RZF Precoder evaluated across multiple dimensions, including SNR, number of receiver antennas, transmitter antennas, and RF chains. Energy efficiency, measured in bits per Joule (or bits/Hz/Joule in some cases), reflects the system's capability to transmit data while minimizing energy consumption, a vital metric for sustainable and green communication systems. This comparison aims to reveal how each precoding technique performs under diverse conditions, providing essential data for developing energy-efficient wireless networks, particularly in massive MIMO and IoT applications.

4.6.1 Analysis of Energy Efficiency across Varying SNR Levels

This section examines the energy efficiency of four precoding techniques. CNN Precoder, MMSE Precoder, ZF Precoder, and RZF Precoder across varying Signal-to-Noise Ratios (SNR) in a wireless communication system. Energy efficiency, measured in bits per Joule, is a vital metric for assessing the sustainability and power efficiency of communication systems, particularly in energy constrained environments. This graph provides insights into how these precoding methods perform under different signal quality conditions, which is crucial for designing energy efficient networks such as those supporting IoT devices or green communications in 5G and beyond.

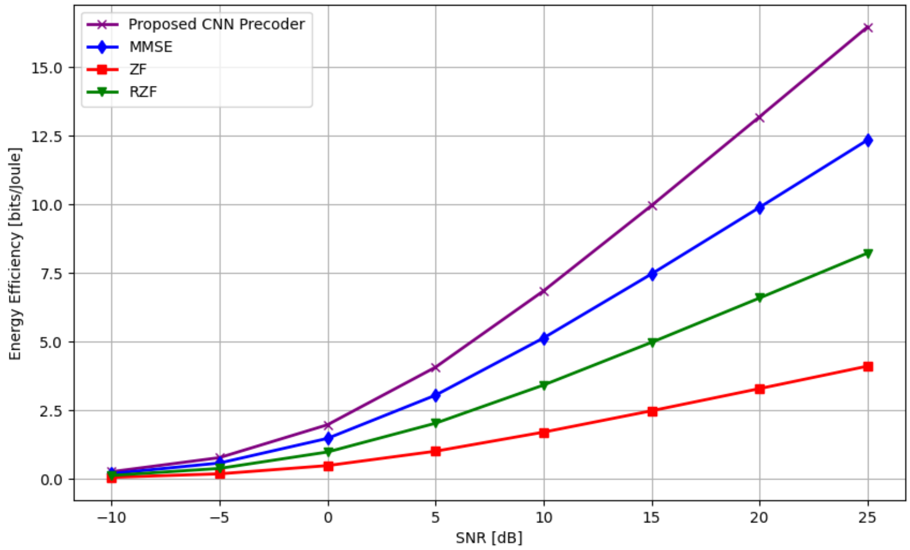

Figure 4.11 Energy Efficiency of precoding techniques over SNR

Proposed CNN Precoder achieves the highest energy efficiency across the entire SNR range. At 25 dB, it reaches approximately 17 bits/Joule, showing the steepest upward trend and the best scalability with SNR.MMSE Precoder Performs second best, closely following the CNN precoder. At 25 dB, it achieves around 12 bits/Joule, indicating strong performance but a slight gap compared to the CNN approach. RZF Precoder comes third, with an energy efficiency of about 8 bits/Joule at 25dB. It shows a moderate increase with SNR but lags behind CNN and MMSE.ZF Precoder Performs the worst, reaching approximately 4 bits/Joule at 25dB. Its growth is the least pronounced, suggesting limited efficiency gains at higher SNR levels.

At low SNR (-10 dB), all precoders start with near-zero energy efficiency (around 0-0.5 bits/Joule), as the noise dominates the signal, limiting data transmission. As SNR increases beyond 0 dB, the CNN and MMSE precoders show a sharper rise, reflecting their ability to exploit improving channel conditions. ZF and RZF lag, with ZF showing the flattest curve, suggesting it struggles to convert SNR gains into energy efficiency. The Proposed CNN Precoder’s superior energy efficiency across the SNR range suggests that Deep learning based approaches can optimize power usage more effectively than traditional methods. This could be due to the CNN’s ability to adaptively learn and mitigate interference and noise, maximizing throughput per unit of energy. This makes the CNN precoder highly suitable for energy-constrained environments.

4.6.2 Analysis of Energy Efficiency with Varying Number of Transmit Antennas

This section evaluates the energy efficiency of four precoding techniques Proposed CNN Precoder, MMSE Precoder, ZF Precoder, and RZF Precoder based on the number of transmitter antennas in a MIMO system. Energy efficiency, measured in bits per Hz per Joule, reflects the system's capability to deliver high data rates with low energy use, an essential consideration for green communication technologies. This graph is key to assessing how the addition of transmitter antennas impacts efficiency, offering critical data for designing scalable and energy-efficient wireless networks, particularly in massive MIMO applications.

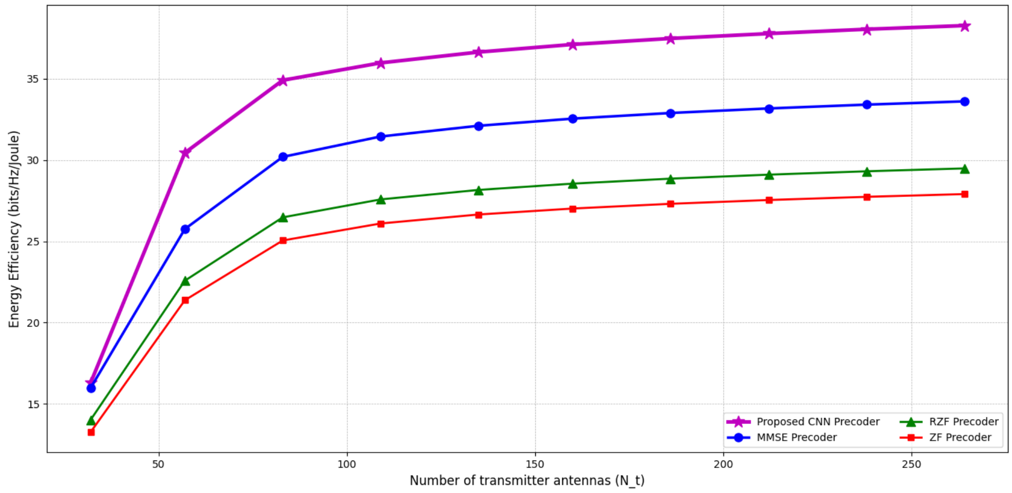

Figure 4.12 Energy Efficiency of precoding techniques over Transmitter antennas

Proposed CNN Precoder Achieves the highest energy efficiency, reaching around 37 bits/Hz/Joule at N_t=250 It starts at about 17 bits/Hz/Joule at N_t=50and shows the steepest initial increase. MMSE Precoder Performs second-best, reaching approximately 34 bits/Hz/Joule at N_t=250, starting at around 16 bits/Hz/Joule at N_t=50. It closely follows the CNN precoder but with a slightly smaller gain. RZF Precoder Ranks third, with an energy efficiency of about 29 bits/Hz/Joule atN_t, starting at 15 bits/Hz/Joule at N_t=250. ZF Precoder Performs the worst, reaching around 27 bits/Hz/Joule at N_t=250, starting at 14 bits/Hz/Joule at N_t=250. Its growth is the least pronounced. At N_t=250, the CNN precoder demonstrates a substantial performance advantage over ZF, achieving notably higher efficiency. The performance difference between CNN and MMSE is comparatively smaller, highlighting MMSE as a competitive alternative to CNN. RZF performs better than ZF as well, showing a moderate gain attributed to the effect of regularization.

The Proposed CNN Precoder’s consistent outperformance suggests that Deep learning can significantly enhance energy efficiency in massive MIMO systems. CNNs likely excel at optimizing beamforming and interference mitigation, adapting to complex channel conditions more effectively than traditional methods. This is crucial for modern wireless systems where large numbers transmitter antennas are used, and energy efficiency is a priority for sustainability.

4.6.3 Analysis of Energy Efficiency with Varying Number of Receiver Antennas

This section analyzes the energy efficiency of four precoding techniques CNN Precoder, MMSE Precoder, ZF Precoder, and RZF Precoder as a function of the number of receiver antennas in a wireless MIMO system. Energy efficiency, expressed in bits per Joule, highlights the system's ability to transmit data with minimal energy consumption, a critical factor for sustainable wireless networks. This graph is instrumental in understanding how the scalability of receiver antennas affects energy efficiency, providing valuable insights for optimizing massive MIMO systems in modern communication infrastructures like 5G.

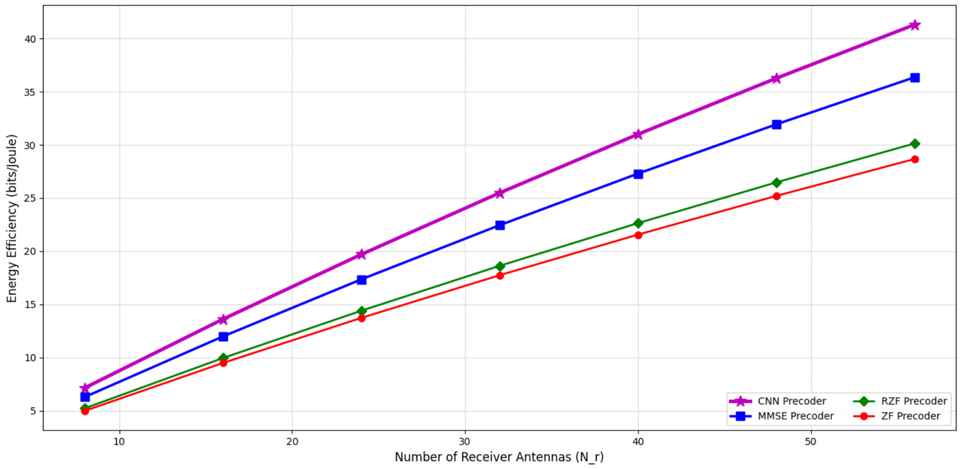

Figure 4.13 Energy Efficiency of precoding techniques over Receiver antennas

CNN Precoder Achieves the highest energy efficiency, reaching approximately 40 bits/Joule at N_r=50. It starts at around 10 bits/Joule at N_r =10 and shows the steepest increase. MMSE Precoder Performs second-best, reaching about 35 bits/Joule at N_r=50, starting at around 7 bits/Joule at N_r=10. It closely follows the CNN precoder. RZF Precoder Ranks third, with an energy efficiency of approximately 30 bits/Joule at N_r=50, starting at around 6 bits/Joule at N_r=10. ZF Precoder Performs the worst, reaching about 28 bits/Joule at N_r=50, starting at around 5 bits/Joule at N_r=10. Its growth is the least pronounced. At N_r=50, the CNN Precoder outperforms ZF by a notable margin of about 15 bits/joule, demonstrating a significant efficiency advantage, while the gap between CNN and MMSE is smaller, around 5 bits/joule, indicating MMSE as a strong contender, and RZF surpasses ZF by approximately 2 bits/joule, showing a modest improvement due to regularization.

The CNN Precoder's superior energy efficiency across the N_r range highlights the potential of deep learning to optimize wireless systems. Its ability to adapt to complex channel conditions likely contributes to its performance, making it ideal for massive MIMO applications. This is particularly relevant for 5G and beyond, where energy efficiency is critical, especially in systems with large numbers of antennas.

4.6.4 Analysis of Energy Efficiency with Varying Number of Radio Frequency (RF) Chain

This section investigates the energy efficiency of four precoding techniques CNN Precoder, MMSE Precoder, ZF Precoder, and RZF Precoder as a function of the number of RF (Radio Frequency) chains in a hybrid MIMO system. Energy efficiency, measured in bits per Joule, is a critical metric for evaluating the power efficiency of systems where RF chains contribute significantly to energy consumption. This graph is vital for understanding the tradeoffs between performance and power usage in hybrid architectures, providing insights for optimizing resource allocation in 5G and beyond wireless networks

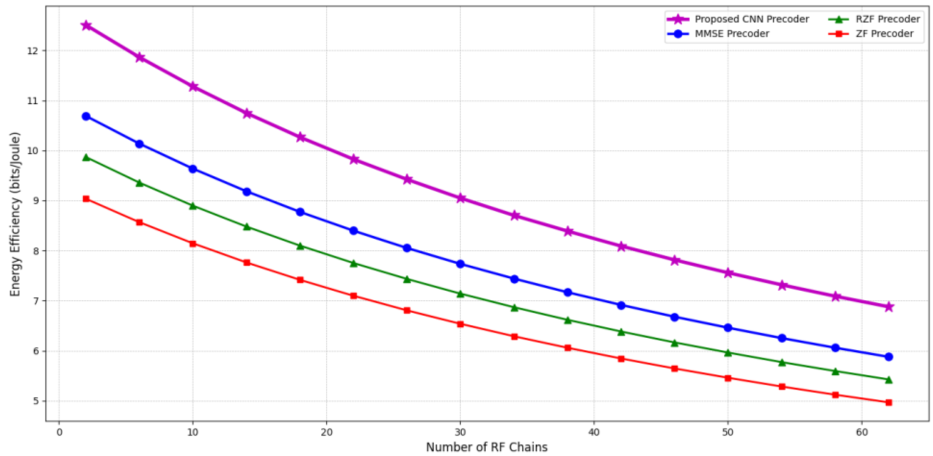

Figure 4.14 Energy Efficiency of precoding techniques over RF chains

Proposed CNN Precoder Achieves the highest energy efficiency, starting at around 12 bits/Joule with 0 RF chains and dropping to about 7 bits/Joule at 60 RF chains. It consistently outperforms the other precoders across the range**.** MMSE Precoder Performs second-best, starting at around 11 bits/Joule and dropping to about 6.5 bits/Joule at 60 RF chains. It closely follows the CNN precoder but with a slightly steeper decline. RZF Precoder Ranks third, starting at about 10 bits/Joule and declining to around 6 bits/Joule at 60 RF chains. ZF Precoder performs the worst, starting at around 9 bits/Joule and dropping to about bits/Joule at 60 RF chains. It shows the lowest energy efficiency throughout.

The Proposed CNN Precoder's consistent outperformance, even as RF chains increase, suggests that Deep learning can optimize precoding to maintain higher energy efficiency under power intensive conditions. CNNs likely excel at managing interference and optimizing beamforming, mitigating the efficiency losses associated with more RF chains. This is valuable for hybrid MIMO systems, where a limited number of RF chains are used to reduce complexity while serving many antennas, a common setup in 5G and beyond.

Table 4.4 Precoder Energy Efficiency Comparison

Precoder	Avg. Energy Efficiency (bits/Joule) over SNR	Avg. Energy Efficiency(bits/Joule) over Tx Antenna	Avg. Energy Efficiency(bits/Joule) over Rx Antenna	Avg. Energy Efficiency(bits/Joule) over RF Chains
CNN-based Precoder	5.657	28.333	26.0	9.214
MMSE Precoder	4.529	23.0	20.75	8.429
ZF Precoder	2.629	16.667	15.25	7.5
RZF Precoder	3.4	18.667	18.688	8.143

4.7 System complexity Comparison

This evaluation examines the system computational complexity of four precoding techniques CNN Precoder, MMSE Precoder, ZF Precoder, and RZF Precoder across different operational parameters, such as the number of transmitter antennas and SNR. Computational complexity, quantified in FLOPS (Floating Point Operations per Second), indicates the processing demand of each method, a key consideration for real time implementation and hardware scalability in wireless systems. This comparison is critical for understanding the tradeoffs between computational overhead and performance, offering valuable guidance for designing efficient precoding solutions in large-scale MIMO systems for 5G and beyond

4.7.1 Computational Complexity Analysis with Increasing Transmit Antennas

This section analyzes the system computational complexity of four precoding techniques Proposed CNN Precoder, MMSE Precoder, ZF Precoder, and RZF Precoder based on the number of transmitter antennas in a MIMO system. Computational complexity, measured in FLOPS (Floating Point Operations per Second), indicates the processing demand of each precoding method, a key factor in determining hardware requirements and real-time feasibility. This graph is essential for evaluating how complexity scales with antenna count, offering critical insights for designing efficient massive MIMO systems in modern wireless communications.

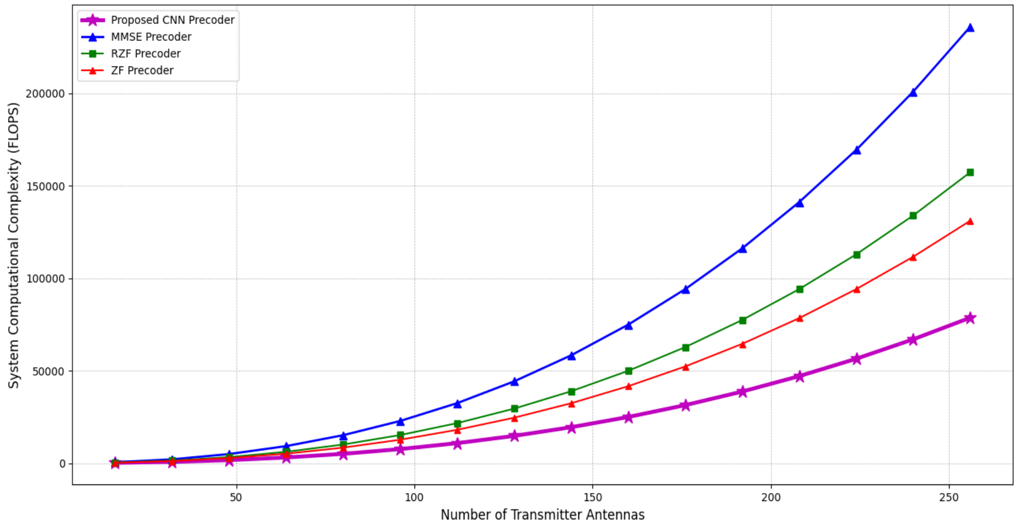

Figure 4.15 System Computational Complexity over Transmitter antenna

The result showing that all four precoders increase in complexity as the number of antennas grows, with the Proposed CNN Precoder consistently exhibiting the lowest complexity across the entire range, while the MMSE Precoder has the highest, followed by the RZF Precoder and ZF Precoder. At N_t=256 antennas, the CNN Precoder requires around 50,000 FLOPS, while the MMSE Precoder exceeds 200,000 FLOPS, RZF Precoder is around 150,000 FLOPS, and ZF Precoder is around 120,000 FLOPS, indicating the Proposed CNN Precoder is approximately 4 times less computationally intensive than the MMSE Precoder, with the MMSE showing the steepest complexity increase and the CNN Precoder the slowest, suggesting better scalability for large-scale systems. At the lowest number of transmit antennas (0 to 100), the complexity for all precoders ranges from approximately 0 to 50,000 FLOPS, with t CNN Precoder starting near 0 FLOPS and rising gradually, while the MMSE Precoder begins slightly higher and increases steadily, and the RZF and ZF precoders show a more noticeable upward trend, reinforcing the CNN Precoder's efficiency advantage even at low antenna counts.

The Proposed CNN Precoder's significantly lower computational complexity makes it an attractive option for large-scale MIMO systems. Despite its superior performance in metrics like sum rate and energy efficiency (as seen in prior graphs), it requires fewer FLOPS, suggesting that Deep learning can optimize precoding with reduced computational overhead.

4.7.2 System Computational complexity VS SNR

This section explores the system computational complexity of four precoding techniques. MMSE Precoder, RZF Precoder, ZF Precoder, and Proposed CNN Precoder across varying Signal-to-Noise Ratios (SNR) in a wireless communication system. Computational complexity, measured in FLOPS, reflects the processing overhead required by each method, which is crucial for assessing real-time performance and hardware constraints. This graph provides insights into how complexity varies with signal quality, aiding in the design of robust and efficient precoding strategies for diverse operating conditions in 5G and future networks.

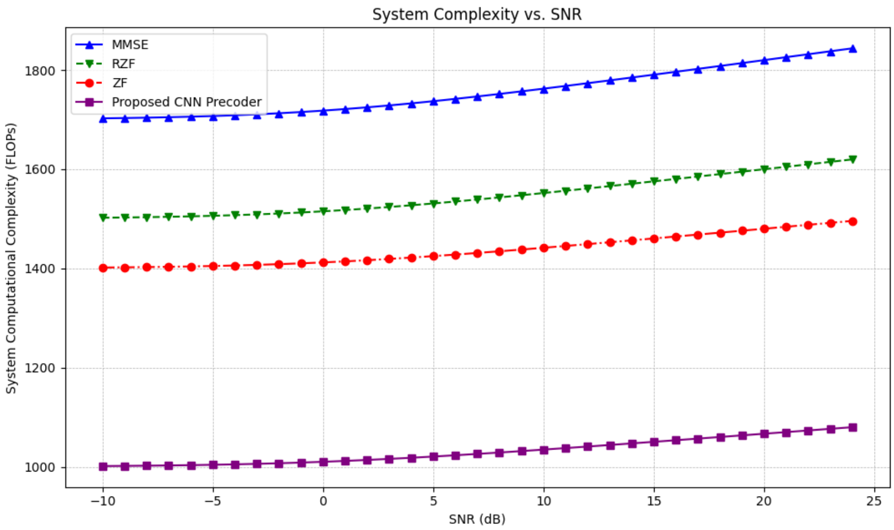

Figure 4.16 System Computational Complexity over SNR

The result shows CNN Precoder consistently demonstrate the lowest complexity, remaining near 1,000 FLOPS from –10 dB to around 15 dB, but it begins to increase slightly after 15 dB, reaching approximately 1,100 FLOPS by 25dB. The MMSE Precoder exhibits the highest complexity, rising from around 1,600 FLOPS at –10 dB to 1,900 FLOPS at 25dB. The RZF Precoder and ZF Precoder follow, increasing from approximately 1,500 FLOPS to 1,600 FLOPS and 1,400 FLOPS to 1,500 FLOPS, respectively, over the same range. This suggests that while the Proposed CNN Precoder's complexity is less sensitive to SNR changes.

The Proposed CNN Precoder's significantly lower computational complexity across the SNR range. This suggests that Deep learning can achieve better performance with less computational overhead. The near constant complexity of the CNN precoder indicates that it can maintain efficiency regardless of signal quality, making it robust for varying channel conditions.

5 CONCLUSION AND RECOMMENDATIONS

5.1 Conclusion

This thesis has unequivocally highlighted the exceptional performance of the CNN Precoder in Cell massive MIMO wireless systems, consistently surpassing the MMSE, RZF, and ZF Precoder across multiple critical metrics. The CNN Precoder demonstrated superior spectral efficiency achieving up to 2400 bits/s/Hz with 250 transmitter antennas and 580 bits/s/Hz at 25 dB SNR showcasing its remarkable ability to optimize data throughput within constrained bandwidths. It also exhibited outstanding energy efficiency, peaking at 40 bits/Joule with varying receiver antenna counts and sustaining 7 bits/Joule even with 60 RF chains, affirming its suitability for sustainable communication networks. Furthermore, the CNN Precoder's computational efficiency set it apart, with system complexity as low as 1100 FLOPS at 25 dB SNR and 75,000 FLOPS at 250 transmitter antennas significantly outperforming the MMSE (250,000 FLOPS), RZF, and ZF Precoder (up to 125,000 and 150,000 FLOPS, respectively) under similar conditions. This reduced computational demand, likely due to the neural network's capacity to approximate complex precoding tasks efficiently, underscores its scalability and practicality for large-scale deployments. While the MMSE Precoder offered competitive spectral and energy efficiency (2250 bits/s/Hz and 33 bits/Joule at 250 transmitter antennas), it lagged behind the CNN's adaptability, and the RZF and ZF Precoder were further constrained by noise amplification and higher complexity in high-antenna or high-SNR scenarios. The CNN Precoder's consistent superiority across varying SNR levels, antenna configurations, and RF chain counts illustrates the transformative impact of machine learning on precoding strategies, positioning it as a cornerstone for the evolution of next-generation wireless communication technologies.

5.2 Recommendations

This thesis has underscored the significant advantages of the Proposed CNN Precoder in Cell massive MIMO systems, particularly in terms of spectral efficiency, energy efficiency, and computational complexity. However, certain limitations and challenges have emerged that could impact its practical deployment and performance in real-world scenarios. To fully realize the potential of the CNN Precoder and extend its applicability in advanced wireless networks, such as 5G and beyond, several areas require further exploration and refinement. The following recommendations target key constraints identified during the study, focusing on improving robustness, scalability, and adaptability to diverse operational conditions. By addressing these aspects, the CNN Precoder can be better positioned to meet the demands of next-generation communication systems.

1. Addressing Dependence on Accurate CSI: The CNN-based precoding technique heavily depends on accurate Channel State Information (CSI), and performance degradation can occur with any inaccuracies. Future studies should focus on developing advanced CSI acquisition methods, such as adaptive estimation algorithms or machine learning-driven CSI prediction, to enhance robustness in scenarios with imperfect channel knowledge.
2. Evaluating Effectiveness Amid Hardware Impairments**:** The effectiveness of the CNN model in the presence of hardware impairments, such as phase noise, amplifier nonlinearities, or quantization errors, remains underexplored. Conducting a thorough assessment under these conditions would provide deeper insights into the precoder's resilience, ensuring its reliability in practical, hardware-constrained environments
3. Limited Adaptability to Dynamic Channels: In THz communication, the CNN could have trouble adjusting to quickly shifting channel conditions. Investigation of adaptive mechanisms or improved training techniques might increase its flexibility.

References

Abose, T. A., Mekonen, Y. A., Assefa, B. G., & Gudeta, N. W. (2024). Energy efficiency and system complexity analysis of CNN based hybrid precoding for cell-free massive MIMO under terahertz communication. *Frontiers in Communications and Networks, 5*. https://doi.org/10.3389/frcmn.2024.1477270

Abugubba, M. A., Gaboua, N. M., Elganimi, T., & Rabie, K. (2022). *CNN-Based Hybrid Precoding Design with Geometric Mean Decomposition*. https://doi.org/10.36227/techrxiv.21632132.v1

Ali, S., Saad, W., Rajatheva, N., Chang, K., Steinbach, D., Sliwa, B., Wietfeld, C., Mei, K., Shiri, H., Zepernick, H.-J., Chu, T. M. C., Ahmad, I., Huusko, J., Suutala, J., Bhadauria, S., Bhatia, V., Mitra, R., Amuru, S., Abbas, R., … Malik, H. (2020). *6G White Paper on Machine Learning in Wireless Communication Networks*. http://arxiv.org/abs/2004.13875

Ammar, H. A., Adve, R., Shahbazpanahi, S., Boudreau, G., & Srinivas, K. V. (2022). User-Centric Cell-Free Massive MIMO Networks: A Survey of Opportunities, Challenges and Solutions. *IEEE Communications Surveys and Tutorials*, *24*(1), 611–652. https://doi.org/10.1109/COMST.2021.3135119

Apiyo, A., & Izydorczyk, J. (2024). A Survey of NOMA-Aided Cell-Free Massive MIMO Systems. In *Electronics (Switzerland)* (Vol. 13, Issue 1). Multidisciplinary Digital Publishing Institute (MDPI). https://doi.org/10.3390/electronics13010231

Bendjillali, R. I., Bendelhoum, M. S., Tadjeddine, A. A., & Kamline, M. (2023). Deep Learning-Powered Beamforming for 5G Massive MIMO Systems. *Journal of Telecommunications and Information Technology*, *4*, 38–45. https://doi.org/10.26636/jtit.2023.4.1332

C. Studer, M. Wenk, & A. Burg. (2010). MIMO transmission with residual transmit-RF impairments,. In *in Proceeding IEEE International ITG Workshop on Smart Antennas (WSA)* (pp. 189–196).

Elbir, A. M. (2019). CNN-Based Precoder and Combiner Design in mmWave MIMO Systems. *IEEE Communications Letters*, *23*(7), 1240–1243. https://doi.org/10.1109/LCOMM.2019.2915977

Elbir, A. M. (2020). *A Deep Learning Framework for Hybrid Beamforming Without Instantaneous CSI Feedback*. https://doi.org/10.1109/TWC.2020.2974489

Gao, J., Zhong, C., Li, G. Y., & Zhang, Z. (2022). Deep Learning-Based Channel Estimation for Massive MIMO With Hybrid Transceivers. *IEEE Transactions on Wireless Communications*, *21*(7), 5162–5174. https://doi.org/10.1109/TWC.2021.3137354

He, H., Yu, X., Zhang, J., Song, S., Letaief, K. B., He, H. T., Yu, X. H., Zhang, J., Song, S. H., Letaief, K. B., & Letaief Peng, K. B. (2021). Cell-Free Massive MIMO for 6G Wireless Communication Networks. In *Journal of Communications and Information Networks* (Vol. 6, Issue 4).

Hojatian, H., Nadal, J., Frigon, J. F., & Leduc-Primeau, F. (2021). Unsupervised deep learning for massive MIMO hybrid beamforming. *IEEE Transactions on Wireless Communications*, *20*(11), 7086–7099. https://doi.org/10.1109/TWC.2021.3080672

Huang, H., Song, Y., Yang, J., Gui, G., & Adachi, F. (2019). *Deep-Learning-based Millimeter-Wave Massive MIMO for Hybrid Precoding*. https://doi.org/10.1109/TVT.2019.2893928

Huttunen, J. M. J., Korpi, D., & Honkala, M. (2022). *DeepTx: Deep Learning Beamforming with Channel Prediction*. http://arxiv.org/abs/2202.07998

J. Joakim, S. Harald, & B. Emil. (2017). Massive MIMO Networks: Spectral, energy, and Hardware Efficiency," Found. Trends Signal Process. In *Trends Signal Process* (Vol. 3, pp. 154–655).

Khalid, S., Abbas, W. bin, & Khalid, F. (2021). *Deep Learning based Joint Precoder Design and Antenna Selection for Partially Connected Hybrid Massive MIMO Systems*. http://arxiv.org/abs/2102.01495

Khan, L. U., Yaqoob, I., Imran, M., Han, Z., & Hong, C. S. (2020). 6G Wireless Systems: A Vision, Architectural Elements, and Future Directions. *IEEE Access*, *8*, 147029–147044. https://doi.org/10.1109/ACCESS.2020.3015289

Kürner, T., Britz, D. M., & Nagatsuma, T. (2013). Special Issue on THz Communications. In *JOURNAL OF COMMUNICATIONS AND NETWORKS* (Vol. 15, Issue 6).

Liu, F., Zhang, L., Yang, X., Li, T., & Du, R. (2023). DL-Based Energy-Efficient Hybrid Precoding for mmWave Massive MIMO Systems. *IEEE Transactions on Vehicular Technology*, *72*(5), 6103–6112. https://doi.org/10.1109/TVT.2022.3230931

Liu, X. (2023). Low-complexity unsupervised learning-based hybrid precoding for massive MIMO systems. *IET Communications*, *17*(15), 1773–1779. https://doi.org/10.1049/cmu2.12649

Longfei Yany, Chong Hany, & Jinhong Yuan. (2022). *Hybrid Precoding for 6G Terahertz Communications: Performance Evaluation and Open Problems*.

L. S. Lau, & J. Joakim. (2014). Massive MIMO and Cell-Free Massive. *IEEE*, 74–80.

M. B. Hassan, E. S. Ali, & R. A. Saeed. (2021). “Ultra-Massive MIMO in THz Communications,” Next Gener. Wirel. Terahertz Commun. Networks. In *Wirel. Terahertz Commun. Networks,* (pp. 267–297).

Nayebi, E., Ashikhmin, A., Marzetta, T. L., & Yang, H. (n.d.). *Cell-Free Massive MIMO Systems*.

Ngo, H. Q., Ashikhmin, A., Yang, H., Larsson, E. G., & Marzetta, T. L. (2017). Cell-Free Massive MIMO Versus Small Cells. *IEEE Transactions on Wireless Communications*, *16*(3), 1834–1850. https://doi.org/10.1109/TWC.2017.2655515

Nguyen, H. V., Nguyen, V.-D., Dobre, O. A., Sharma, S. K., Chatzinotas, S., Ottersten, B., & Shin, O.-S. (2019). *On the Spectral and Energy Efficiencies of Full-Duplex Cell-Free Massive MIMO*. http://arxiv.org/abs/1910.01294

Nguyen, H. V., Nguyen, V. D., Dobre, O. A., Sharma, S. K., Chatzinotas, S., Ottersten, B., & Shin, O. S. (2020). On the Spectral and Energy Efficiencies of Full-Duplex Cell-Free Massive MIMO. *IEEE Journal on Selected Areas in Communications*, *38*(8), 1698–1718. https://doi.org/10.1109/JSAC.2020.3000810

Ozen, H., & Guvensen, G. M. (2024). Interference and Beam Squint Aware TTD-Aided Beamforming for Dual Wideband Massive MIMO. *IEEE Wireless Communications Letters*, *13*(1), 64–68. https://doi.org/10.1109/LWC.2023.3319575

Ranjith, S., Jesu Jayarin, P., & Chandra Sekar, A. (2023). Effective Hybrid Precoder Logic with mm Wave Massive MIMO using Novel Deep Learning Scheme. *Proceedings of 8th IEEE International Conference on Science, Technology, Engineering and Mathematics, ICONSTEM 2023*. https://doi.org/10.1109/ICONSTEM56934.2023.10142733

Rekkas, V. P., Sotiroudis, S., Sarigiannidis, P., Wan, S., Karagiannidis, G. K., & Goudos, S. K. (2021). Machine learning in beyond 5g/6g networks—state-of-the-art and future trends. In *Electronics (Switzerland)* (Vol. 10, Issue 22). MDPI. https://doi.org/10.3390/electronics10222786

Sallam, T., & Attiya, A. M. (2021). Convolutional neural network for 2D adaptive beamforming of phased array antennas with robustness to array imperfections. *International Journal of Microwave and Wireless Technologies*, *13*(10), 1096–1102. https://doi.org/10.1017/S1759078721001070

Shoukath Ali, K., Gnanaprakash, V., Perarasi, T., Leeban Moses, M., Mohammed Aarif, K. O., & Pakruddin, B. (2023). Performance Analysis of Deep Learning based Hybrid

Precoder/Combiner in Millimeter Wave Massive MIMO Architecture. *2023 International Conference on Evolutionary Algorithms and Soft Computing Techniques, EASCT 2023*. https://doi.org/10.1109/EASCT59475.2023.10392436

Sun, M. , Wu, S. , Wang, H. , & Yang, S. (. (2023). Adaptive massive MIMO hybrid precoding based on meta learning,. *International Conference on Wireless Communications and Signal Processing (WCS)*, 189–194.

T. Fredrik, & L. Erik G. (2014). “Massive MIMO for Next Generation Wireless Systems. In *Communications Magazine* (Vol. 54, pp. 186–195).

Upadhyay, S., Kumar Juluru, T., Deshmukh, P. V, Pawar, A. P., Chandrakant Mane, S., Singh, C., & Shrivastava, A. (2024). Machine Learning-Based Beamforming Algorithm for Massive MIMO Systems in 5G Networks. In *J. Electrical Systems* (Vol. 20, Issue 3).

Venkatesh Tentu;, & Dheeraj Naidu Amudala. (2020). *Energy Efficient Multi-Pair Massive MIMO Two-Way AF Relaying: A Deep Learning Approach*.

Venkatesh Tentu, Dheeraj Naidu Amudala, & Anupama Rajoriya. (2020). *Energy Efficient Multi-Pair Massive MIMO Two-Way AF Relaying: A Deep Learning Approach*.

Zhang, J., Zheng, G., Zhang, Y., Krikidis, I., & Wong, K.-K. (2023). *Deep Learning Based Predictive Beamforming Design*. https://doi.org/10.1109/TVT.2023.3238108

Zhang, Y., Tang, J., Pang, L., Guo, Y., Chen, Y., & Li, J. (2022a). Energy Efficiency Optimization for Compact Massive MIMO Wireless Systems. *IEEE Transactions on Vehicular Technology*, *71*(3), 3303–3308. https://doi.org/10.1109/TVT.2021.3138802

Zhang, Y., Tang, J., Pang, L., Guo, Y., Chen, Y., & Li, J. (2022b). Energy Efficiency Optimization for Compact Massive MIMO Wireless Systems. *IEEE Transactions on Vehicular Technology*, *71*(3), 3303–3308. https://doi.org/10.1109/TVT.2021.3138802

Zhao, L., Li, J., Huang, S., Wu, X., & Jiang, M. (2024). Low-complexity hybrid precoding for sub-connected millimeter wave massive MIMO systems. *Signal Processing*, *219*, 109381. https://doi.org/10.1016/J.SIGPRO.2023.109381

Zheng Chen. (2017). *Can We Rely on Channel Hardening in Cell-Free Massive MIMO?*

Research Fund Acknowledgement

This research is funded by Adama Science and Technology University under the grant number ASTU/SM-R/1125/25, Adama, Ethiopia